484

ENGINEERING EXPERIMENT STATION

Georgia Institute of Technology

PROJECT INITIATION

Date January 26, 1960

PROJECT TITLE: Alterations of the MILORD Mine Watch Radar

PROJECT NO: A-484

PROJECT DIRECTOR: A. L. Hollimon

SPONSOR: Dept. of The Navy, Office of Naval Research

EFFECTIVE: 1-1-60 ESTIMATED TO RUN UNTIL: 4-30-60

TYPE AGREEMENT: Basic Contract No. Nonr 3084(00)
and Contract No. Nonr-3084(01)X

Amount: $73,000.00
Reports: Final Report - not later than 7-31-60
Others - As required by Scientific Officer
Contact Person: Director
Naval Research Laboratory
Washington 25, D. C.
(Scientific Officer)

Assigned to Radar Branch - Electronics Divsion

Copies to:

- ☐ Project Director
- ☐ Director
- ☐ Associate Director
- ☐ Assistant Director(s)
- ☐ Division Chiefs
- ☐ Branch Head
- ☐ Accounting
- ☐ General Office Services
- ☐ Rich Electronic Computer Center
- ☐ Purchasing
- ☐ Engineering Design Services
- ☐ Technical Information Section
- ☐ Photographic Laboratory
- ☐ Shop
- ☐ Security Officer
- ☐ Report Section
- ☐ Library ✓

EES FORM 400 (Rev 7-59)

Final Report
Project No. A-484

REDESIGN OF THE MILORD ANTENNA

- o - o - o - o -

Department of the Navy
Office of Naval Research
Contract No. Nonr-3084(01)(x)

- o - o - o -

30 November 1960

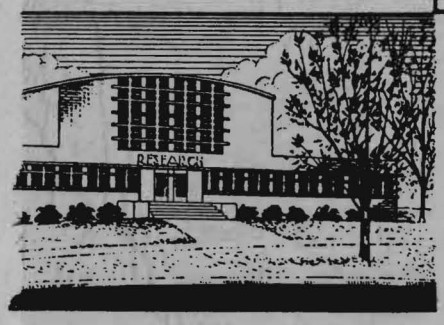

Engineering Experiment Station
Georgia Institute of Technology
Atlanta, Georgia

ENGINEERING EXPERIMENT STATION
of the Georgia Institute of Technology
Atlanta, Georgia

Final Report
Project No. A-484

REDESIGN OF THE MILORD ANTENNA

Prepared by

A. L. Holliman

Object: Performance of Research and Development for Altering the Characteristics of the MILORD Antenna

30 November 1960

TABLE OF CONTENTS

LIST OF FIGURES

ABSTRACT

Redesign of the MILORD Radar Antenna (developed at Georgia Tech in 1953-54 for the Department of the Navy under Contract No. NObsr 64055) has been conducted by the Georgia Tech Engineering Experiment Station on Contract Nonr-3084(01)(X). The design and development of a microwave ring switch, four pillbox primary feeds, and a steering mechanism was performed in order to alter the electrical characteristics of the antenna as shown below.

	Before Modification	After Modification
Frequency (mc)	9375	9050
Bandwidth (mc)	190	1000
Polarization	Horizontal	Vertical
Scan-Sector (degrees)	85	40
Scan-Sector Steering Angle (degrees)	0	143
Scan rate (scans/sec)	4,8, or 16	8 or 16
Peak Power (kw)	250	300
Azimuth Half-Power Beamwidth (degrees)	0.75	0.74
Elevation Half-Power Beamwidth (degrees)	3.5	3.65
Gain (db)	40	39
Azimuth Side-Lobe Level (db)	- 19	- 17-1/4
Elevation Side-Lobe Level (db)	--	- 21

This report describes the design and development program conducted during the modification of the antenna, and it discloses the electrical characteristics of the modified antenna.

PURPOSE OF CONTRACT

The purpose of this contract, Nonr-3084(01)(X), was to redesign the MILORD (Mine Impact LOcating Radar Device) experimental mine-watch radar antenna which was designed and developed at Georgia Tech in 1953-54 for the Department of the Navy under Contract No. NObsr 64055. The original characteristics of this system were described in Equipment Characteristics of the MILORD Mine-Watch Radar, Report No. A-129/T4, 30 September 1955, Engineering Experiment Station, Georgia Institute of Technology (ASTIA No. AD302468). The MILORD antenna was also described in "An X-Band Wide Angle Scanner", by Hollis and Holliman, Record of the Georgia Tech-SCEL Symposium on Scanning Antennas, December 1956, Engineering Experiment Station, Georgia Institute of Technology (ASTIA No. AD 132769).

The design objectives for the modified antenna were as follows:

Frequency	9050 mc
Bandwidth	1000 mc
Scan Sector	40 degrees and steerable
Polarization	Vertical
Beamwidth, horizontal	3/4 degree
Beamwidth, vertical	3-1/2 degrees
Peak Power	300 kw
Scan Rate	8 or 16 scans/sec.

I. INTRODUCTION

In order to modify the antenna to meet the design objectives, it was necessary to perform the following operations: the design and development of a microwave switch and four pillbox primary feeds to replace the corresponding components on the original MILORD antenna, the design and construction of a motor-driven gear drive for remotely positioning the microwave switch and a synchronization unit in order to relocate the azimuthal position of the scan sector of the antenna, and the replacement of the RG-52/U waveguide with RG-51/U waveguide in order to provide the desired power-transmitting capability.

This report describes the design and development program conducted during the modification of the antenna (under Georgia Tech Research Project No. A-484 and Department of the Navy Contract No. Nonr-3084(01)(X)), and it discloses the characteristics of the modified antenna.

II. GENERAL DESCRIPTION

The modified MILORD antenna assembly, shown in Figures A and B, consists of four identical offset parabolic-cylinder reflectors of aluminum mounted back-to-back and equally spaced on a common hub, each with a line-source primary feed which establishes vertical polarization. The primary feeds are of the "pillbox" or "hoghorn" type, each consisting of a parabolic reflecting barrier between closely spaced aluminum plates with a sectoral feed at the focal point of the parabolic barrier. Each of these feeds is sequentially energized by a microwave switch as its reflector rotates into the active scan sector of the antenna. The vertical apertures of the reflectors are enclosed with fiberglas honeycomb radomes; the tops and bottoms of the parabolic cylinders are enclosed with aluminum honeycomb panels. This construction transforms the antenna assembly into a smooth right-circular cylinder which substantially reduces the power required to rotate it. The resulting cylinder is 14 feet in diameter and 32 inches in height; it weighs approximately 6,000 pounds, rotates at speeds of 120 or 240 RPM, and has a moment of inertia of approximately 2700 slug-feet^2 about its axis of rotation.

As the antenna rotates, a 40-degree azimuth sector is scanned at either 8 or 16 scans per second with a vertically polarized 0.74 x 3.65 degree beam (azimuth x elevation) having a gain of 39 db and a frequency band of 8550 mc to 9550 mc; the center of this scan sector can be remotely reoriented in azimuth throughout a 143 degree sector, which is centered with respect to the rear of the trailer. All interconnecting waveguide used in the antenna and ring switch assembly is RG-51/U.

A trailer, constructed of welded steel channel and mounted on tandem wheels, supports the spindle, antenna, and drive motor, and makes the

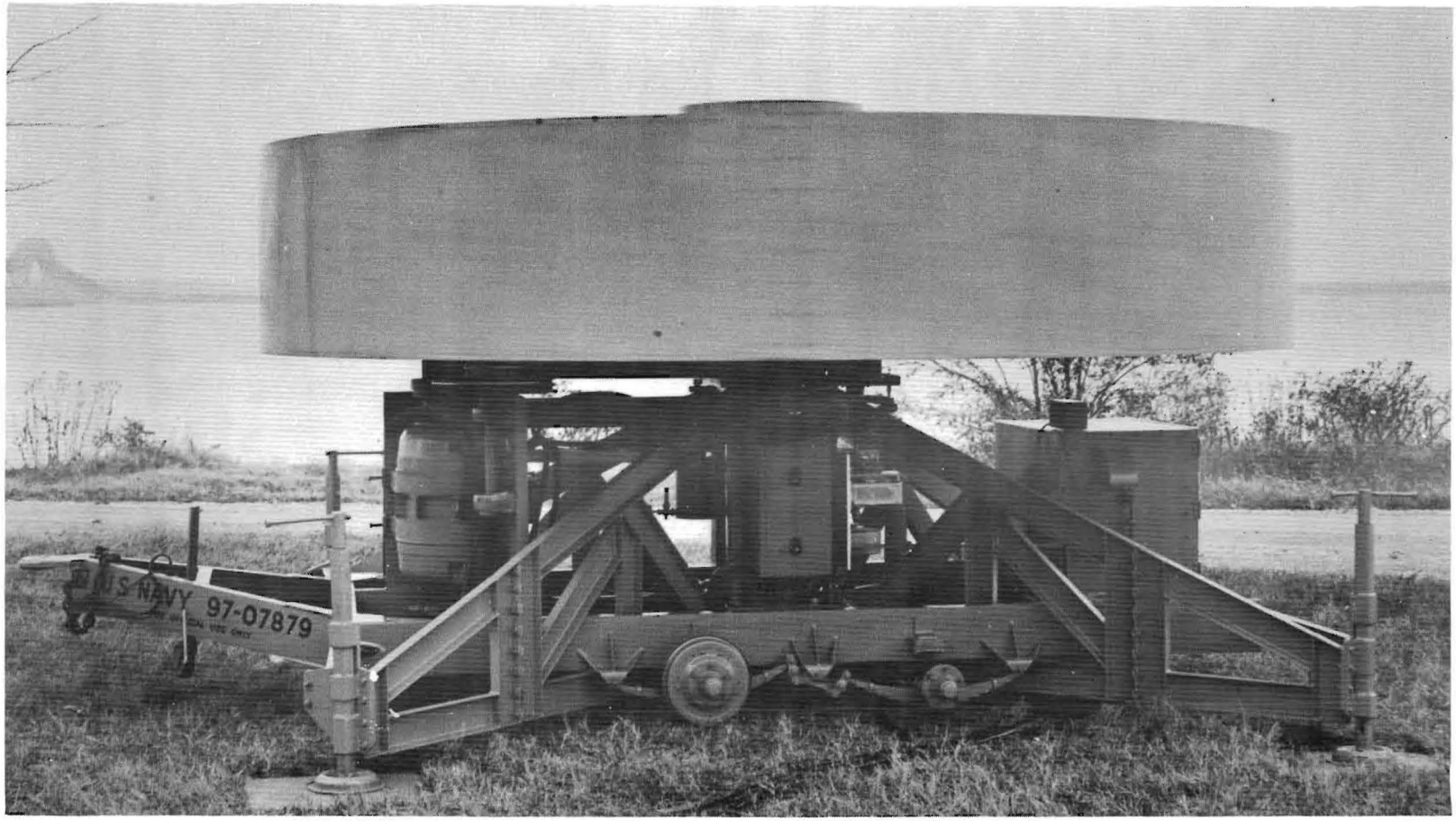

Figure A. The MILORD Antenna.

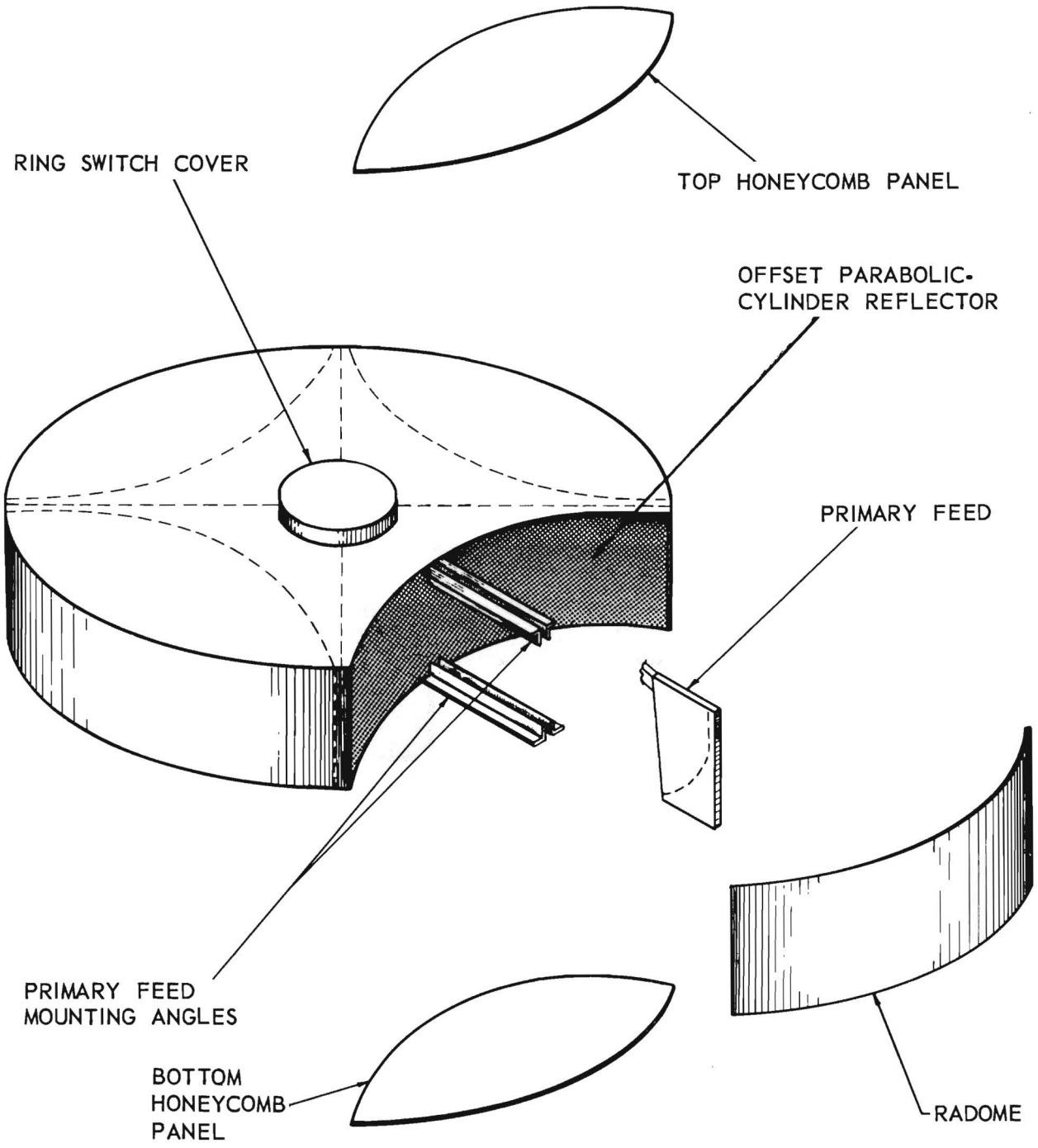

Figure B. Exploded View of Major Antenna Components.

assembly portable. Removable outriggers and jacks provide a stable support for the trailer during antenna operation. A shaft, gear-driven from the antenna and rotating at twice the speed of the antenna, is provided on the trailer below the antenna for driving a synchronization unit. A system consisting of shafts, gears, cams, switches, a turntable, and an electric motor is provided for remotely positioning the synchronization unit and the microwave switch simultaneously in order to relocate the azimuthal position of the scan sector of the antenna.

III. PRIMARY FEED, REFLECTOR, AND RADOME

3-1. Pillbox Primary Feed

Collimation of the antenna beam in a vertical plane is produced by a pillbox primary feed (see Figures C and D); the feed also provides the proper illumination for the parabolic-cylinder reflector which collimates the antenna beam in a horizontal plane. The feed has a vertical aperture of 24-3/16 inches and produces conical wavefronts having a 2° apex half-angle. Each feed consists of a parabolic reflecting barrier located between parallel conducting plates which have a separation equal to the H-plane dimension of RG-51/U waveguide. The barrier is fed at its focus with a small E-plane sectoral horn. The reflecting barrier is asymmetrical, being the section of a parabolic cylinder extending from its vertex to a point near one end of its latus rectum. An output-horn configuration, located along the linear aperture of the pillbox, provides the proper illumination for the reflector.

The design of the primary feed involved six basic problems: the design of an E-plane sectoral horn with the proper radiation pattern; the design of a parabolic reflecting barrier; the alignment of the center-of-phase of the sectoral horn with the focal point of the parabolic reflecting barrier; the design of an output-horn configuration along the linear aperture of the feed; the orientation of the latus rectum of the parabolic barrier at the proper angle with respect to the linear aperture; and the reduction of reflections produced by discontinuities in the pillbox by means of impedance matching.

3-1.1. Parabolic Reflecting Barrier

Since the height of the offset cylindrical reflector was established when it was originally constructed, the overall height of the pillbox primary feed

$\alpha = 2°$

$\beta = 2.46°$

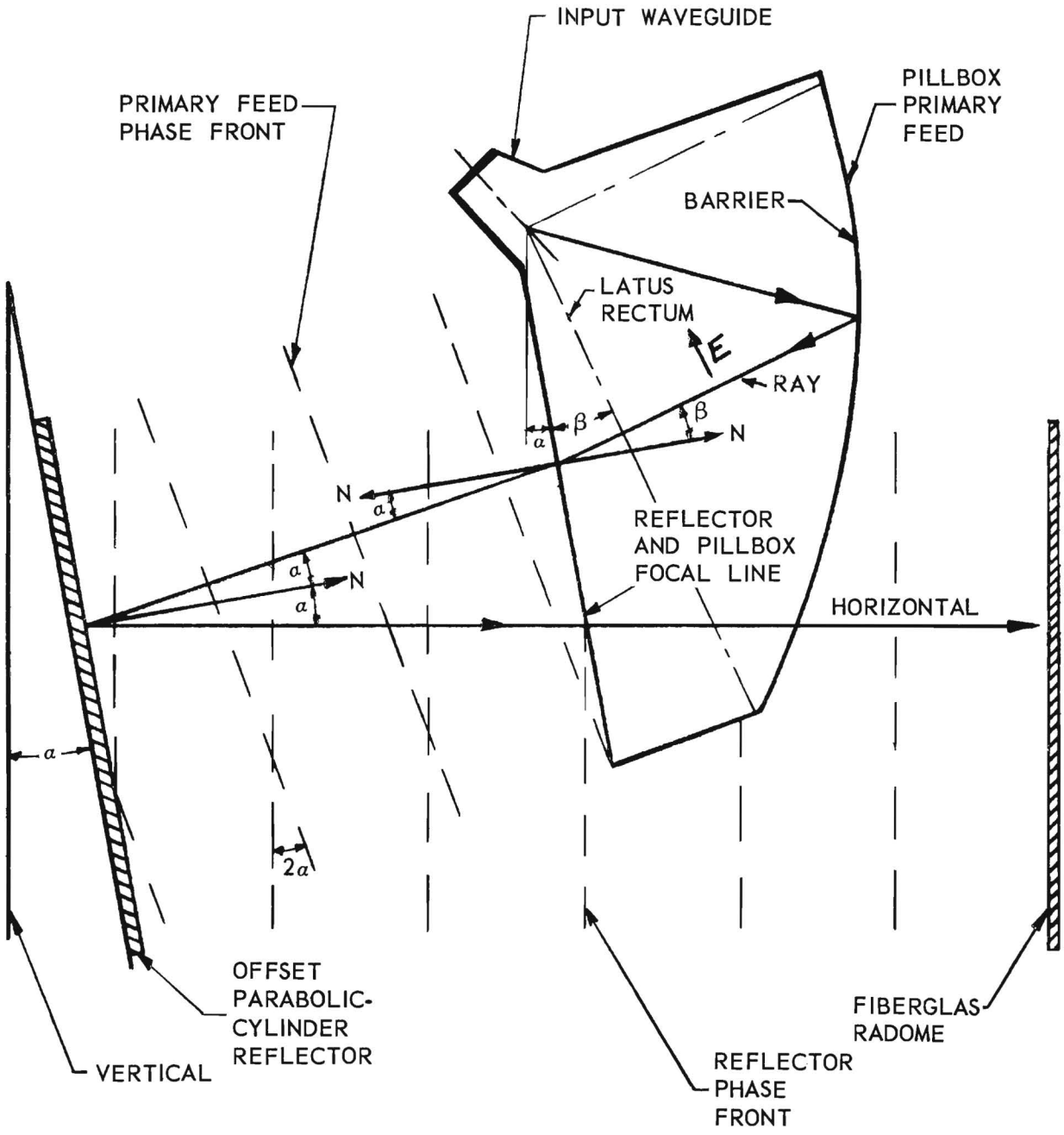

Figure C. A Schematic Vertical Cross Section Through the Pillbox Primary Feed, the Offset Parabolic Cylinder Reflector, and the Fiberglas Radome.

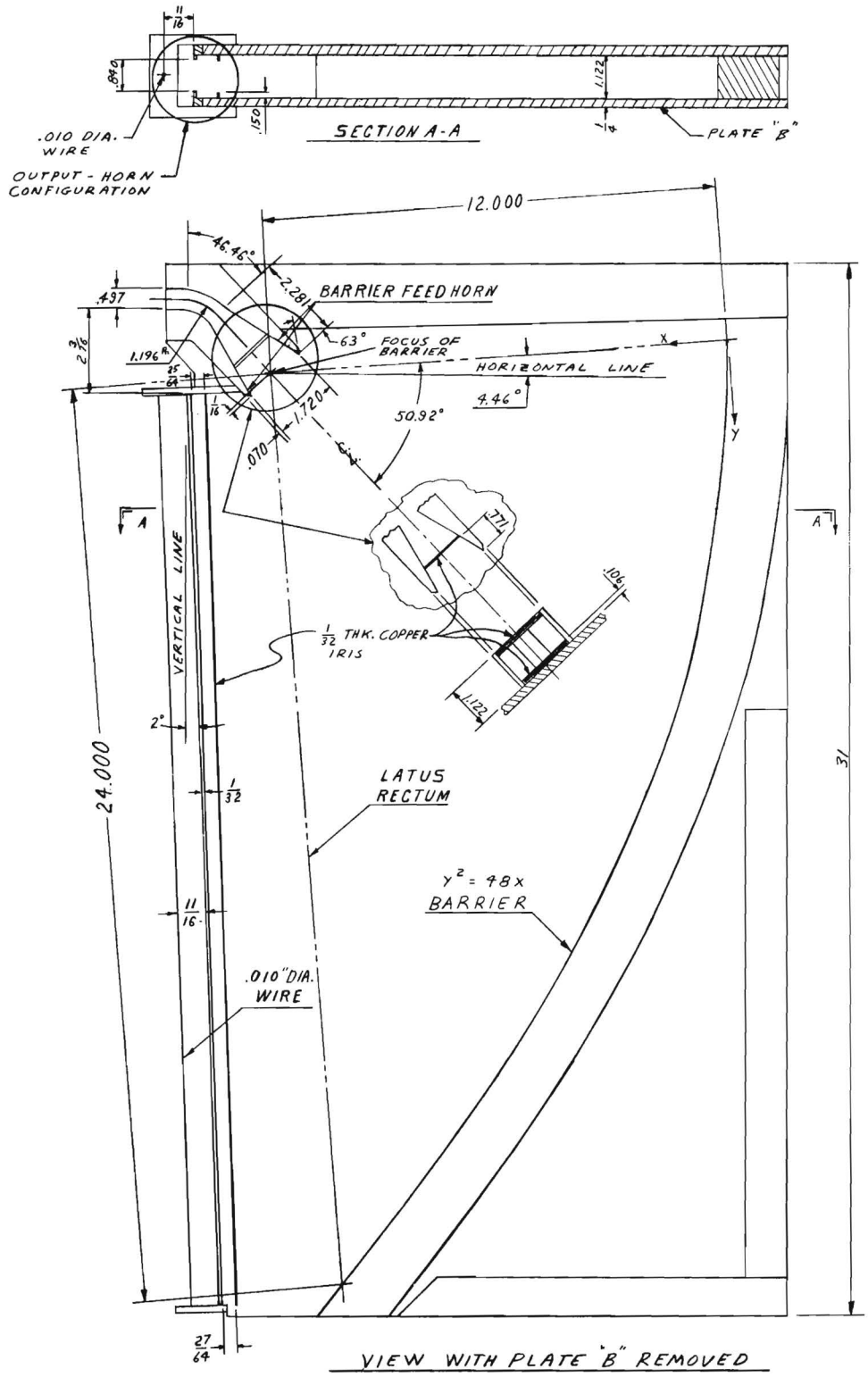

Figure D. Construction Details of a Pillbox.

was limited to that of the original pillbox of 31 inches; the maximum possible focal length of the barrier was limited since the pillbox was required to be on the axis of the parabolic reflector and to be restrained between the previously established focal line of the reflector and the fiberglas radome. It was thus decided to use the same parabolic contour for the barrier as was previously used ($y^2 = 4fx = 48x$). The width of the barrier, which determined the spacing between the parallel conducting plates of the pillbox, was increased and made equal to the H-plane dimension of RG-51/U waveguide (1.122 inches) to prevent cutoff with vertical polarization and to eliminate the need for a taper between the pillbox and the waveguide. (The RG-51/U waveguide had been selected to replace the RG-52/U waveguide, that was previously used, in order to increase the power-transmitting capability of the antenna to the specified 300 kw peak).

3-1.2. E-Plane Sectoral Horn

Since the use of a reflecting barrier having the same contour as that used in the original MILORD antenna had been selected, it was then considered desirable to design an E-plane sectoral barrier feed-horn that would have approximately the same radiation pattern as that possessed by the original H-plane sectoral barrier feed-horn (see Appendix A). It was believed that the far-zone elevation radiation pattern, which would be produced by the combination of this barrier feed-horn and the parabolic reflecting barrier, would then have approximately the same characteristics of main-beam width and side-lobe level with vertical polarization at 9050 mc as the original antenna possessed with horizontal polarization at 9375 mc; (this was one of the design objectives).

A full-scale model of the original H-plane sectoral barrier feed-horn was made, and its radiation pattern was measured while it radiated between parallel conducting plates (having the same spacing of 0.400 inch as the parallel plates of the original pillbox) at a frequency of 9375 mc with its electric field polarized perpendicular to the plates (which corresponded to the polarization orientation between the parallel plates of the pillbox of the original horizontally-polarized antenna). Calculations were then made to determine the approximate horn-aperture dimension required (having a correspondingly small aperture phase variation) to produce a similar radiation pattern when radiating between the parallel plates (having a spacing of 1.122 inches as proposed for the new pillbox) at 9050 mc with polarization parallel to the plates (which corresponded to the polarization orientation required between the parallel plates of the pillbox being designed to provide the antenna with vertical polarization).

A horn was constructed having this calculated E-plane aperture dimension and having a small E-plane flare angle (to reduce its aperture phase variation to the relative magnitude of that of the original H-plane horn). The horn's E-plane radiation pattern was then measured between parallel plates and compared with the above measured radiation pattern of the original horn. The horn's aperture dimension was then altered slightly to obtain approximate pattern correspondence; the radiation patterns of the H-plane and the E-plane sectoral horns are shown in Figure R. (The fringe effects of the electromagnetic field at the edges of the aperture of each horn limited the accuracy with which the new horn-aperture dimension could be calculated, and thus it was necessary to resort to the "cut-and-try" method to refine their pattern correspondence.)

3-1.3. Barrier and Feed-Horn Alignment

In order to properly align the center-of-phase of the barrier feed-horn with the focus of the parabolic reflecting barrier, a full scale model of each was made and installed between parallel plates to produce a configuration approximating that of the final pillbox. A temporary horn was mounted along the linear output aperture of the pillbox to reduce the impedance mismatch between the parallel plates and free space; a jig was constructed to allow the positioning of the feed horn relative to the barrier while maintaining the center line of the horn coincident with the focus of the barrier and oriented at a predetermined angle with respect to the latus rectum of the barrier (see Figure D). (This angle was 39-1/12 degrees, approximately the same as used in the original pillbox, which gave a compromise between having the location of the peak of illumination at the center of the vertical aperture of the pillbox and having equal illumination at its edges.) The far-zone elevation patterns of the pillbox model were then measured for various locations of the focus of the barrier relative to the aperture of the horn; the horn was then permanently located at the position that gave the most symmetrical main-beam shape having maximum side-lobe suppression.

3-1.4. Output Horn

Since the contour of the parabolic-cylinder reflector had been established in the original design and construction of the MILORD antenna, it was impractical, and also unnecessary, to attempt to modify it. It was thus considered desirable to design a pillbox output-horn that would have approximately the same azimuth radiation pattern at 9050 mc when polarized parallel to the parallel plates of the pillbox (vertical polarization) as the original pillbox output-horn had at 9375 mc when polarized perpendicular to the parallel plates (horizontal

polarization) (see Appendix B). It was believed that the antenna far-zone azimuth radiation pattern, which would be produced by the combination of this output horn and the reflector, would then have approximately the same characteristics of main-beam width and side-lobe levels as those of the original antenna (this was one of the design objectives).

A full-scale model of a one-inch-high section of the output horn of the original pillbox was made. (This could be simulated by cutting a section from the pillbox by two horizontal cross-sectional cuts, separated vertically by one inch, through the output horn and the parallel plates of the pillbox.) The radiation pattern of this horn model was measured while radiating between parallel plates spaced one inch apart at a frequency of 11,085 mc. This frequency was used to provide the same wavelength between the parallel plates, with polarization parallel to them, as the free-space wavelength at 9375 mc that existed in the vicinity of the aperture of the output horn of the original pillbox.

A similar full-scale model of a one-inch-high section of the output horn of the proposed pillbox was made; since this horn was formed by the parallel plates of the pillbox only, it was thus unflared. The radiation pattern of this horn model was also measured while radiating between the above parallel plates at 9050 mc with polarization perpendicular to them.

The radiation pattern produced by the unflared horn model was found to have a beamwidth much smaller than that of the horn model of the original pillbox. It was not possible to decrease the horizontal aperture dimension of the proposed pillbox enough to sufficiently increase this beamwidth since, with vertical polarization (E-field parallel to the pillbox parallel plates), the wave atten-

uation increases rapidly as the horizontal aperture (H-plane dimension) decreases toward $\lambda/2$ and the wave is cutoff for apertures equal to or less than $\lambda/2$. (λ is the free-space wavelength and the TE_{10} mode is assumed to exist in the pillbox.)

It was thus necessary to resort to an experientally-determined output-horn configuration that would produce an increased beamwidth without decreasing the pillbox aperture below cutoff. This configuration was obtained by a slight abrupt reduction in the horizontal aperture of the pillbox (from 1.122 inches to 0.840 inch) and by centrally locating a vertical conducting steel wire of 0.010 inch diameter at a distance of 11/16 inch in front of the pillbox aperture (see Figure D).

The resultant radiation of this horn configuration has a wide beamwidth due to the interacting radiation patterns of two antennas (the plane-aperture antenna formed at the output of the pillbox parallel plates, and the parasitic wire antenna, which is energized by radiation from the plane aperture). This pattern was found to be a function of the width of the plane aperture and of the diameter, location, and conductivity of the wire.

3-1.5. Orientation of Pillbox's Barrier with Its Aperture

The reflectors of the original MILORD antenna were constructed as parabolic cylinders having a vertical offset angle α of 2° (see Figure C); it was thus necessary that the focal line of each pillbox (which is located parallel to, and in the vicinity of, the pillbox aperture) be coincident with the focal line of the offset parabolic cylinder for proper focusing. It was also necessary that the conical wavefronts produced by the pillbox have an apex half-angle of 2° with respect to the pillbox aperture; then, vertical-plane phase fronts would be produced after reflection by the reflector, and the center line of the

elevation beam of the antenna would be oriented in a horizontal plane (this was a desired objective).

During transmission, the barrier of the pillbox transforms the cylindrical wavefronts produced by its feed horn into plane wavefronts which are oriented parallel to its latus rectum. These plane wavefronts must approach the linear aperture of the pillbox at an angle β such that, after refraction at the aperture (due to an apparent change in the index of refraction of the transmission medium caused by a different phase velocity in the pillbox from that in free space outside the pillbox), the emergent wavefronts will make an angle α of 2° with the aperture. The angle β was calculated to be 2.46° and the pillbox was constructed so that its linear aperture was oriented at this angle with respect to the latus rectum of its barrier (see Appendix C).

3-1.6. Impedance Matching

Sources of reflections exist at the discontinuties at the aperture of the barrier feed horn, at the surface of the parabolic reflecting barrier, and at the wire and metal strips comprising the output horn at the aperture of the pillbox.

The reflections produced at the aperture of the feed horn and at the surface of the barrier were matched with an inductive iris located inside the throat of the feed horn. Reflections from the pillbox aperture were prevented during this matching operation by temporarily extending the parallel plates at the aperture and then inserting a load made of wood, which had a gradual linear taper in the H-plane (the taper began at the inside surface of one plate and extended to the inside surface of the other plate in order to have it originate and terminate in regions of low field intensity). A reference plane was obtained by temporarily locating a metal short across the

waveguide at the input to the pillbox. The iris was temporarily supported inside a block of styrofoam and then inserted inside the throat of the feed horn during the initial matching operation. After the location and dimensions of the iris had been determined by calculation and then checked by experiment, the metal strips composing the iris were permanently secured within slots machined in the feed-horn members.

The reflections produced at the pillbox aperture were then matched with an inductive iris located inside the parallel plates near the aperture. A reference plane was obtained by temporarily locating a metal short across the aperture; the iris was temporarily supported inside a strip of styrofoam and then inserted between the parallel plates. After the dimensions and the location of the iris had been determined, the metal strips composing the iris were permanently secured within slots machined in the parallel plates.

Inductive irises were used, rather than capacitive irises, in order to permit maximum possible power-transmitting capability. The dimensions and locations of the matching irises are shown in Figure D, and curves of VSWR versus frequency over the design band for the pillboxes are shown in Figure E.

The elevation and azimuth patterns of the redesigned pillbox are shown in Figures F and G.

3-2. Reflector

3-2.1 General Description

The reflector is an offset parabolic cylinder with its axis making an angle of α with the vertical. The orientation of the primary feed and the reflector is such as to produce a vertical plane wavefront in the aperture of the reflector; the dimensions of this aperture are approximately 108 x 24 inches (horizontal x vertical).

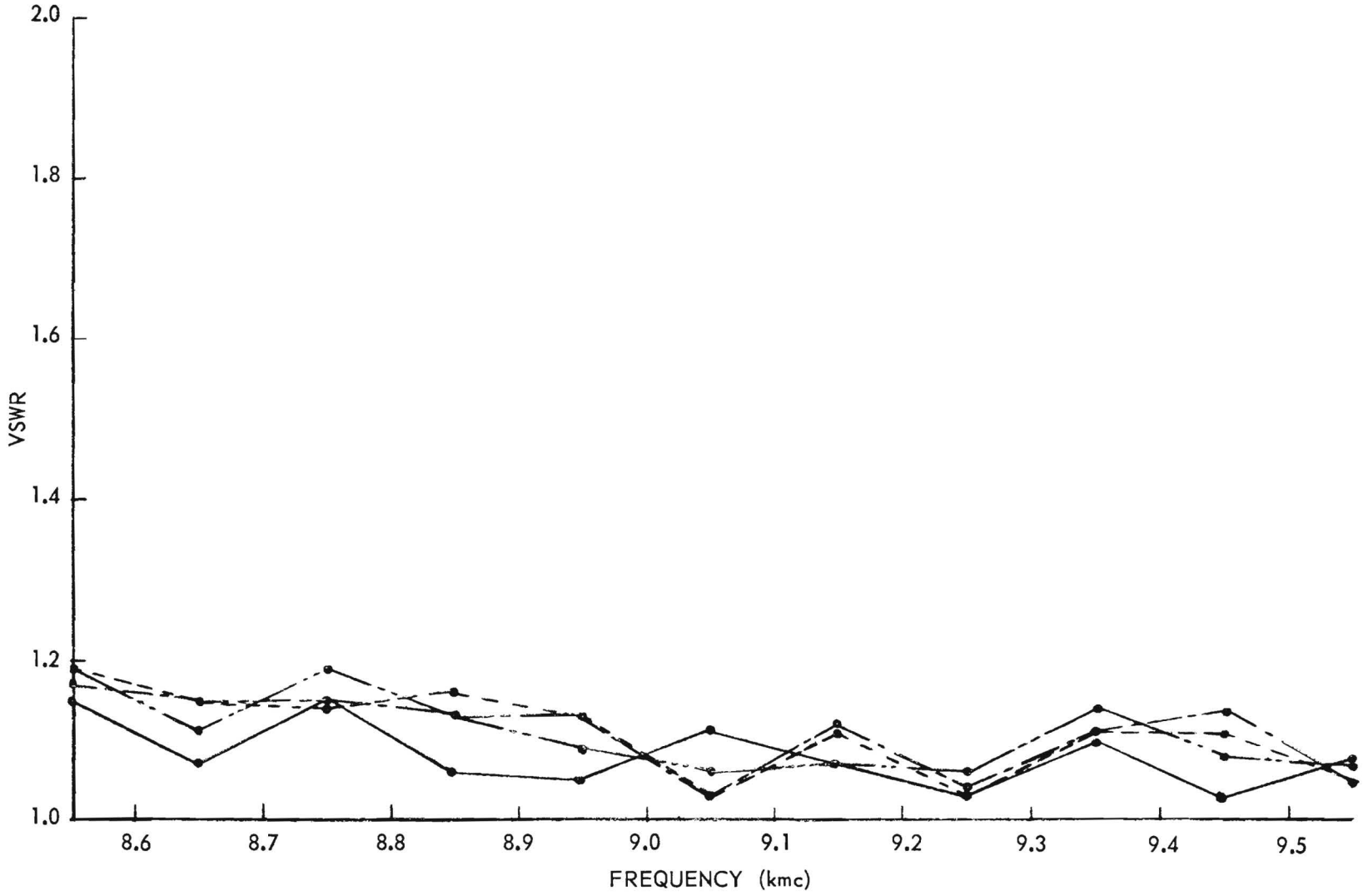

Figure E. VSWR Versus Frequency Curves for the Four Pillboxes Radiating into Free Space.

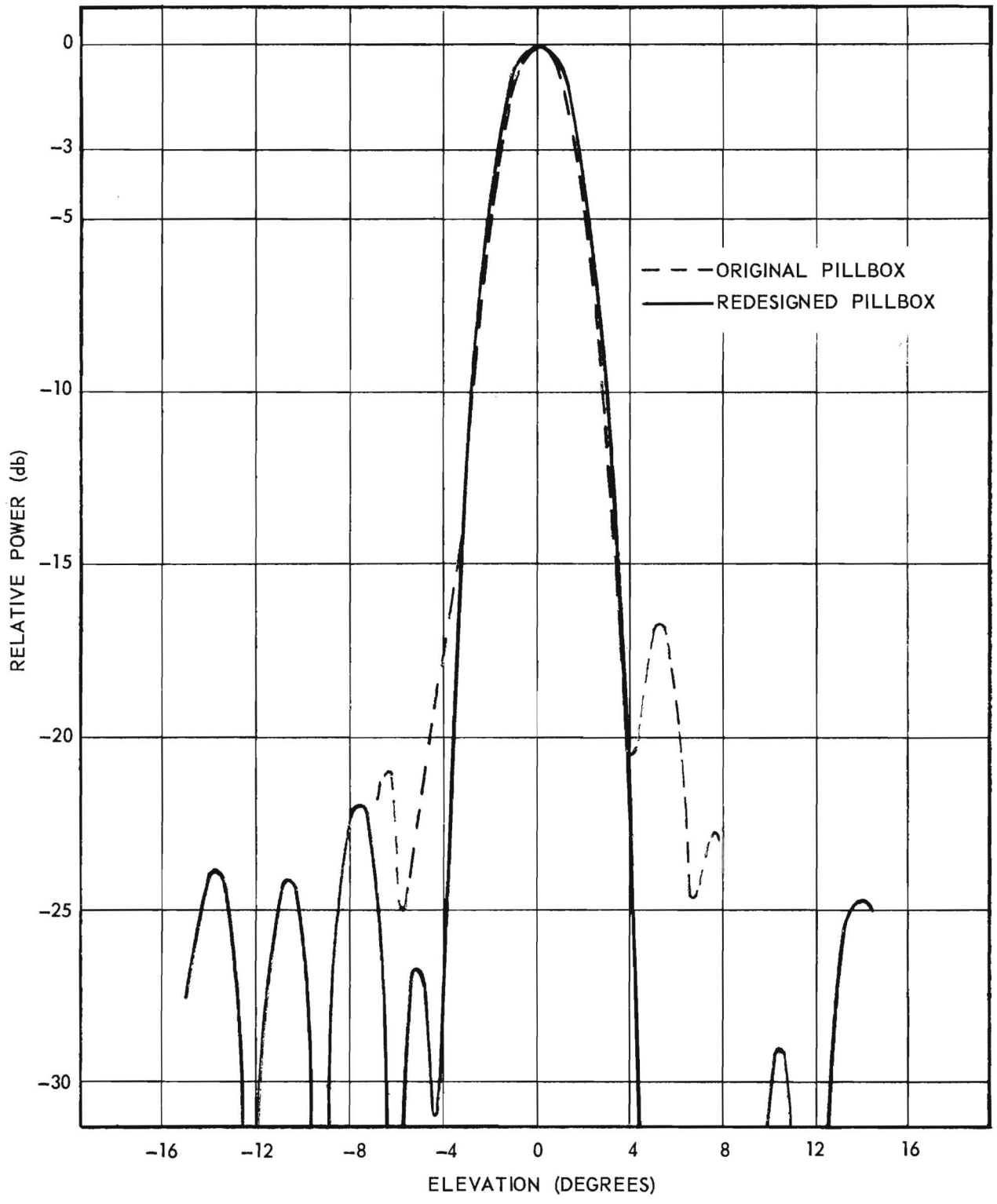

Figure F. A Typical Pillbox Elevation Radiation Pattern.

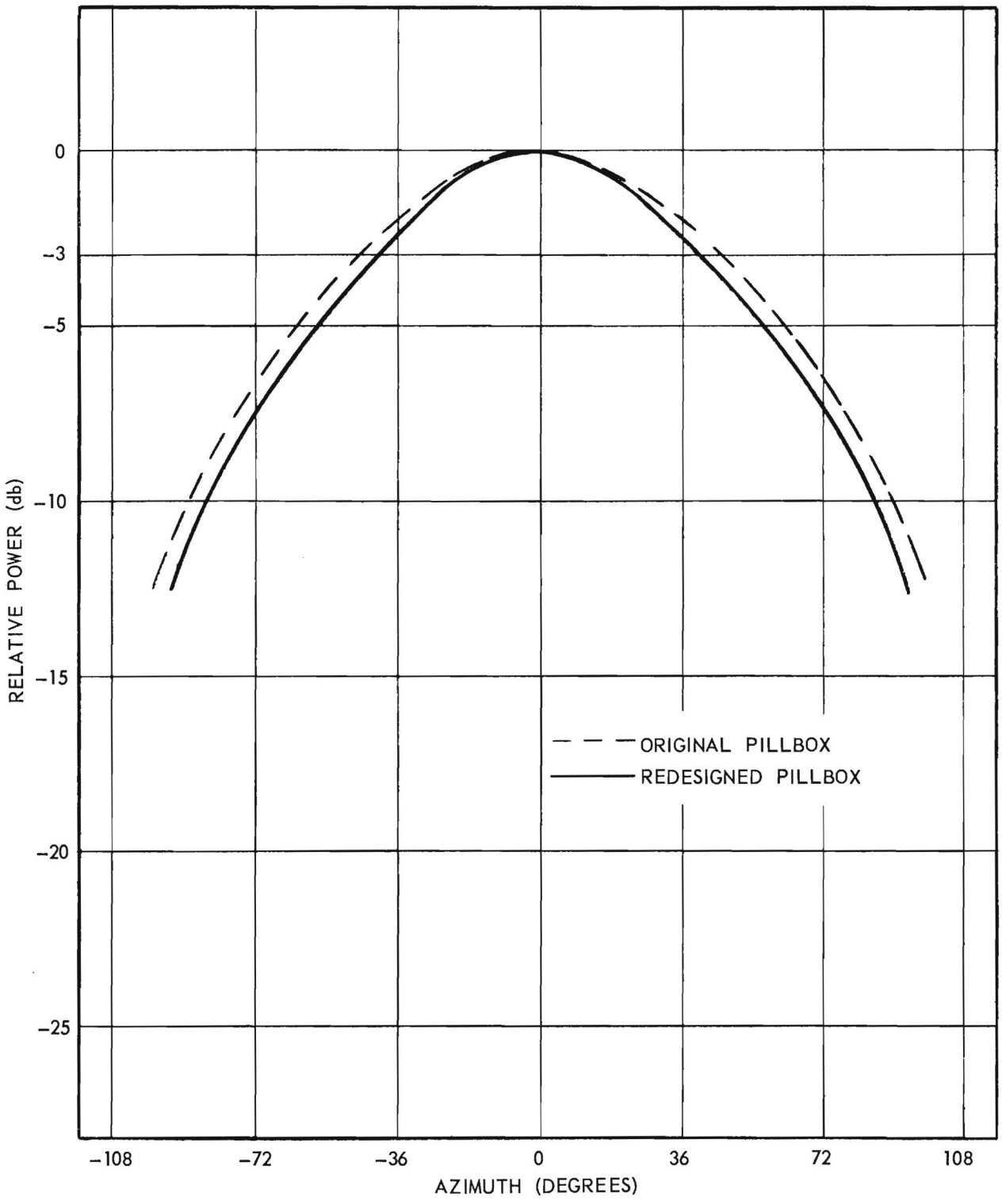

Figure G. A Typical Pillbox Azimuth Radiation Pattern.

3-2.2. Offset Orientation

To reduce the energy reflected from the surface of the parabolic-cylinder reflector back into the mouth of the primary feed during transmission, the axis of the parabolic cylinder had been previously offset from the vertical by an angle α (see Figure C). To provide for proper focusing, the center-line-of-phase of the output horn of the line-source pillbox feed was located coincident with the focal line of the reflector; thus, the aperture of the pillbox had the same angle of tilt α with the vertical as the axis of the cylinder. The barrier was oriented between the parallel plates of the pillbox so that its latus rectum, and also its reflected phase front during transmission, made an angle β with the pillbox aperture and its center-line-of-phase. The angle β was selected such that, after refraction at the aperture, the emergent phase fronts from the pillbox were concentric cones, each having an apex half-angle of α and having its axis coincident with the center-line-of-phase. After collimation and reflection by the reflector, the transmitted phase fronts became parallel vertical planes which oriented the center line of the radiated beam into a horizontal plane. Note that the phase fronts of the reflector make an angle of 2α with those of the pillbox; thus, energy reflected from the reflector back into the pillbox during transmission appears to arrive from a direction in the elevation plane of 2α relative to the center line of the elevation beam of the pillbox. The angle α was originally selected so that 2α was approximately equal to the angular position of the first null, measured with reference to the center line of the beam; thus, by employing an offset primary feed and reflector, the energy reflected back into the feed was reduced. On the modified antenna α was 2° (required to be the same as on the original antenna since the original

reflector was used without modification), and β was calculated to be 2.46 degrees (see Appendix C).

The energy reflected back into the pillbox by the reflector was attenuated more than 25 db. A further advantage of this method of offsetting the feed was the fact that reflections back into the waveguide from the discontinuity at the line-source aperture of the pillbox feed were attenuated in a similar manner.

3-3. Radome

The original fiberglas radome was used on the modified antenna. It is a normal-incidence sandwich-type radome, characterized by a low value of reflection coefficient over a wide frequency band, low loss, excellent rigidity, and small differential phase delay with angle of incidence.

The original design parameters for the radome included a two-percent frequency band centered at 9375 mc and polarization of the E-field in a horizontal plane; however, it was found to be satisfactory for use at 8550 mc to 9550 mc with vertical polarization.

After installation of the primary feed, antenna radiation patterns were measured without and with the fiberglas radome installed; these patterns are shown in Figure H for a frequency of 9050 mc. The one-way reduction in power transmission with the radome installed was measured and found to be less than 1/3 db with a negligible degradation in beam shape and side-lobe suppression.

3-4. Assembly

3-4.1. Pillbox-Reflector Alignment

During the assembly process, antenna radiation patterns were measured; each pillbox was centered with respect to the vertical axis-plane of its cylindrical reflector and positioned radially (while maintaining its aperture

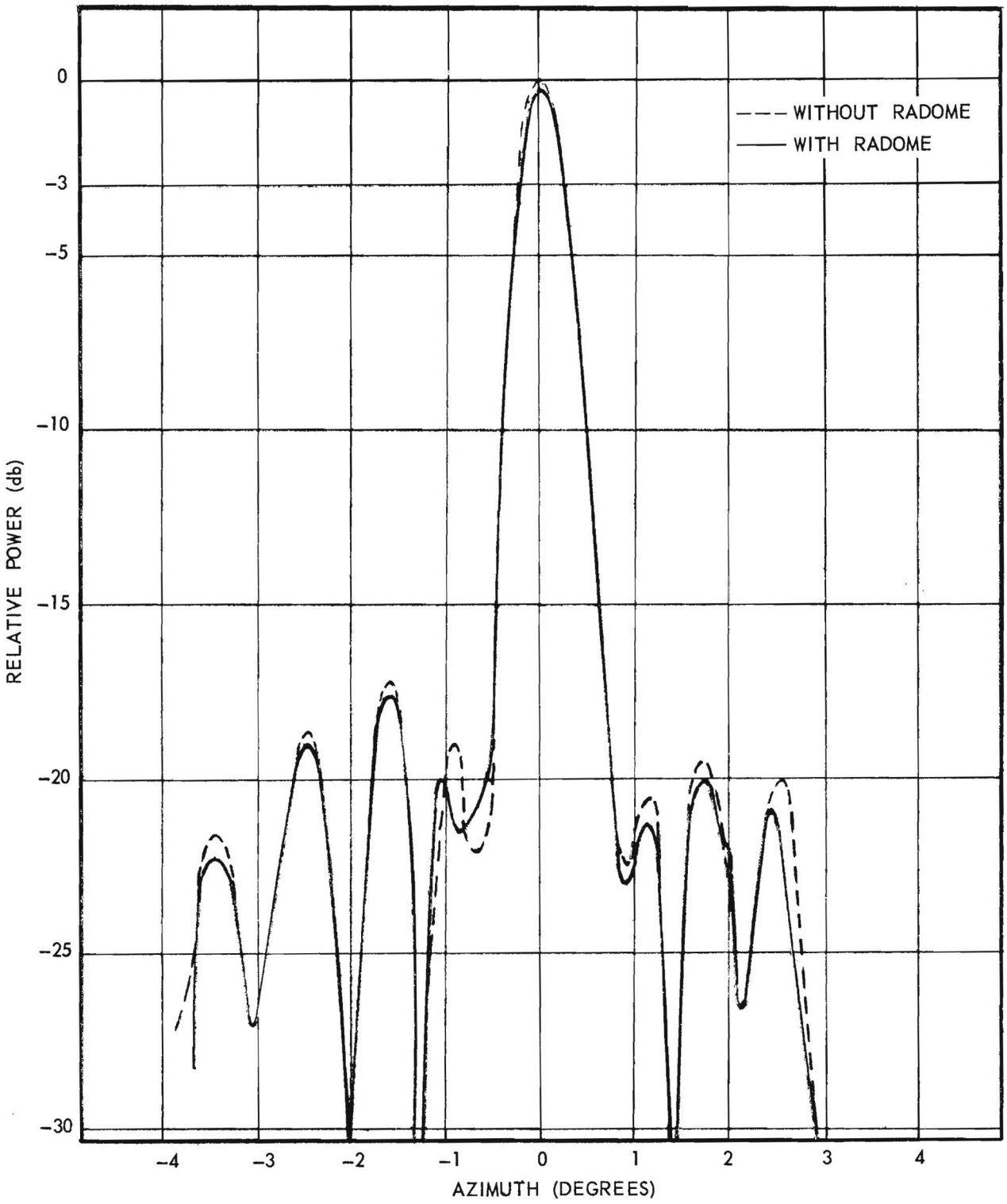

Figure H. Antenna Azimuth Radiation Patterns With and Without the Fiberglas Radome Installed (f = 9050 mc).

parallel to the focal line of the reflector) until a beam pattern having minimum practical side lobes was obtained. It was then assumed that the center-line-of-phase of the pillbox output-horn was coincident with the focal line of the reflector. While maintaining the above reflector-pillbox separation as their mean separation distance, each pillbox was rotated slightly, as required, in the axis-plane until the center line of the elevation beam of its reflector was located in a horizontal plane. Each pillbox was then moved perpendicular to the axis-plane, as required, in order to obtain 90° azimuthal spacing between the center lines of the radiated beams of the four pillbox-reflector assemblies.

The elevation beam center lines of the four assemblies were vertically oriented into a horizontal plane with a tolerance of less than ± 1/16 degree and the azimuth center lines were equally spaced in a horizontal plane with a tolerance of less than ± 1/20 degree.

3-4.2. Antenna Beam Characteristics

A typical azimuth beam pattern and elevation beam pattern are shown in Figures I and J respectively. The half-power azimuth beamwidth is 0.74 ±0.01 degrees, and the half-power elevation beamwidth is 3.65 ±0.10 degrees. In the azimuth plane, the maximum side-lobe level is 17-1/4 db below the amplitude of the main beam. Due to the physical size and weight of the antenna, it was not possible to obtain more than the main-beam portion of the elevation patterns; however, since the reflector essentially acts as a plane mirror for the elevation beam (which is collimated by the pillbox primary feed), it can be assumed that the side-lobe suppression of the elevation beam for the reflector will be practically the same as that for the pillbox (see Figure F). The maximum side-lobe level in the elevation plane would then be approximately 21 db below the amplitude of the main beam.

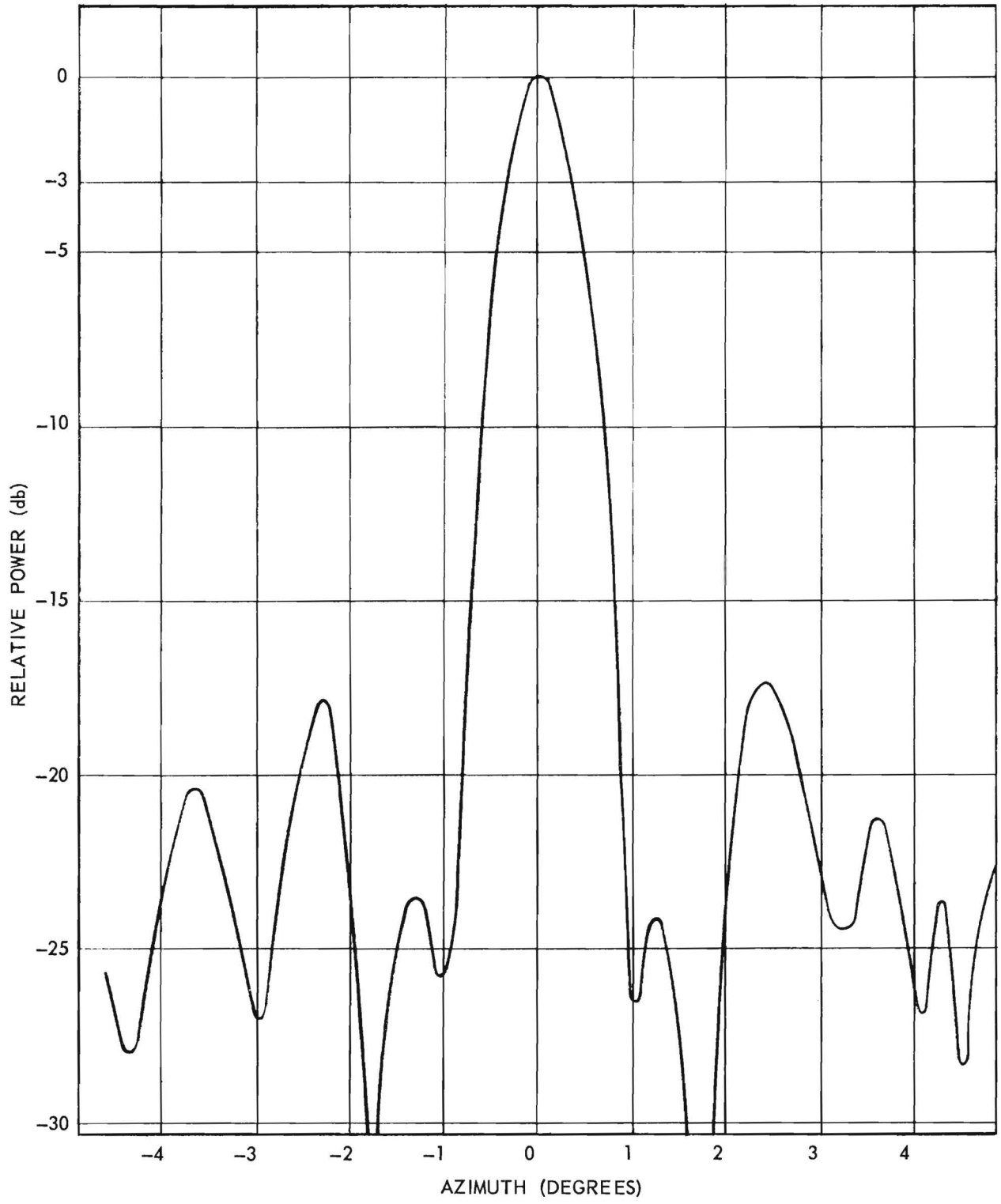

Figure I. A Typical Antenna Azimuth Radiation Pattern (f = 9050 mc).

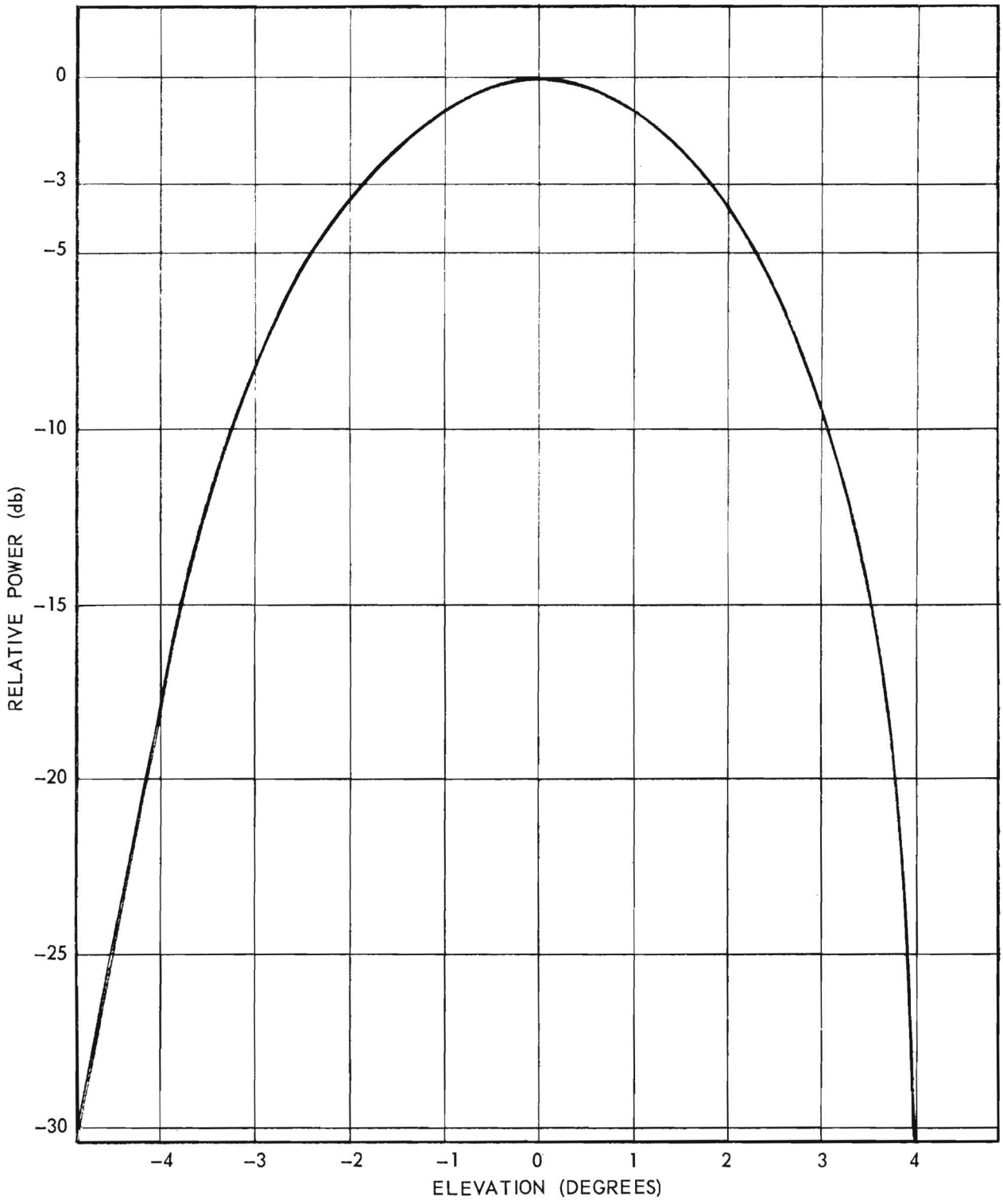

Figure J. A Typical Antenna Elevation Radiation Pattern (f = 9050 mc).

The peak gain of the antenna, relative to an isotropic radiator, was obtained by comparison with the gain of a standard-gain horn. The gain of all four assemblies was found to be 39 ± 1/3 db. The estimated gain of the antenna, as obtained from the measured half-power beamwidths in the azimuth and elevation planes, was 40-1/2 db (see Appendix F).

3-4.3. Antenna Impedance Characteristics

The VSWR for each of the four pillbox-reflector-radome assemblies was measured at representative frequencies throughout the design band; these curves are shown in Figure K. The energy transmission path consisted of the following components (see Figure B): (1) the switch-pillbox waveguide which included a 90° H-plane bend, an offset including two H-plane bends, and a 90° twist; (2) the pillbox which included an E-plane bend, the E-plane barrier feed horn, the parallel plate medium, the parabolic reflecting barrier, and the output-horn configuration; (3) the offset parabolic-cylinder reflector; and (4) the fiberglas honeycomb radome.

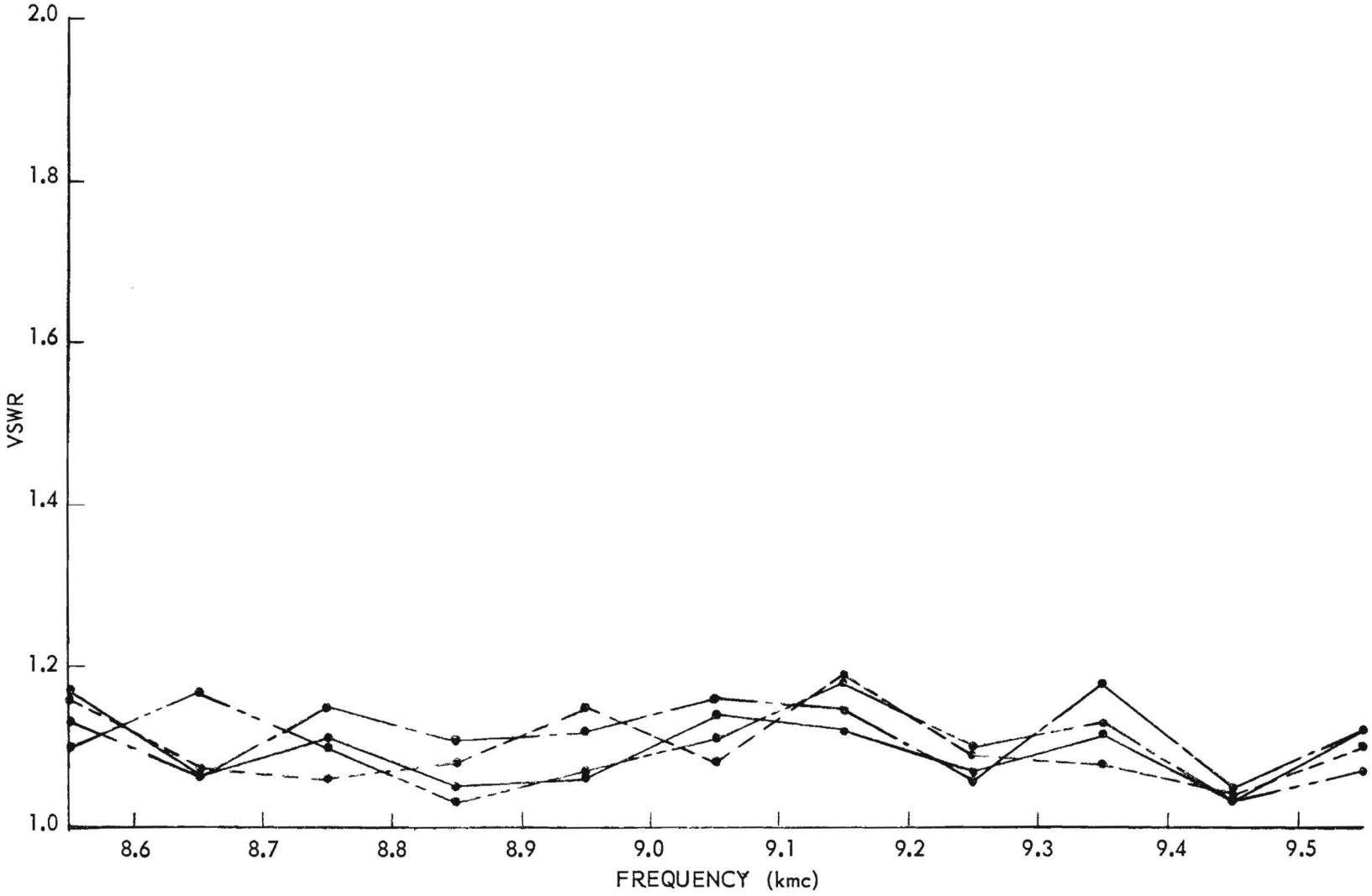

Figure K. VSWR Versus Frequency Curves for the Four Pillbox-Reflector-Radome Assemblies.

IV. MICROWAVE SWITCH AND WAVEGUIDE

4-1. Microwave Switch

4-1.1. General Description

The purpose of the microwave switch is to feed energy successively to each of the four pillboxes of the antenna as the beam of its reflector rotates through the scan sector; a ring switch was designed and developed for use with the MILORD antenna for this purpose. The switch operates at 9050 mc and has low-loss and low-reflection characteristics over its design bandwidth of 1000 mc. These characteristics were made possible by the use of the offset junction which was developed at Georgia Tech under Contract Nos. DA 36-039 SC-72789 and DA 36-039 SC-74870. This junction is described in "A Waveguide Switch Employing the Offset Ring-Switch Junction" by Johnson, Holliman, and Hollis, I.R.E. Transactions on Microwave Theory and Techniques, September 1960, pages 532-37.

This ring switch is a device for sequentially switching energy from a stationary waveguide into one of four circularly-moving waveguides; a section through the switch is shown in Figure L. Its basic structure consists of two rectangular ring waveguides, each of which is split longitudinally down the center of its H-dimension to allow one portion of each guide to rotate relative to its other portion. Energy is coupled into, between, and out of these two split waveguides by means of offset waveguide junctions and waveguide bends.

4-1.2. Principle of Operation

Although the switch is a bilateral device, the following description is written on the assumption that it is directing energy from a microwave transmitter to the antenna. Energy is coupled from the input waveguide

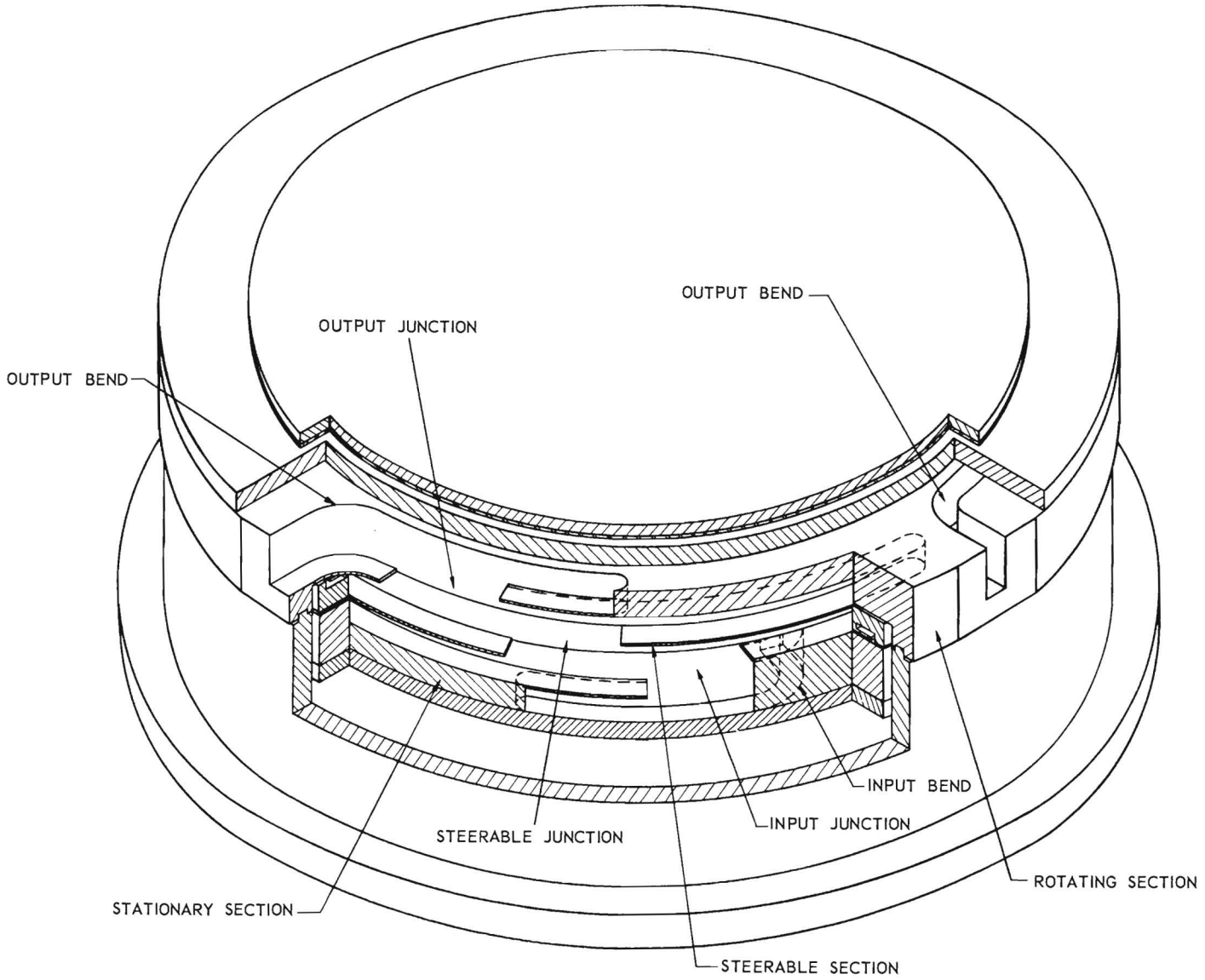

Figure L. A Section Through the Microwave Ring Switch.

bend into the lower ring guide (which is stationary) by the input junction. The energy flows through this ring guide until it reaches the junction in the steerable center section of the switch; it is then coupled into the upper ring guide and flows through this guide until it reaches an output junction located in the rotating section of the switch. This junction couples the energy into the output bend from which it is directed to the connected pillbox and reflector (then located in the azimuthal scan sector); as the antenna rotates, successive output junctions are energized while their connected pillbox and reflector rotate through the 40° scan sector. The angular location of the scan sector, relative to the angular position of the input waveguide, can be remotely reoriented within a 143° sector; this reorientation is achieved by rotating the steerable center section of the switch which changes the angular position of its junction relative to the stationary input junction.

Note that energy can travel in only one direction around the ring after it has been coupled into a ring guide; propagation in the other direction is prevented by an abrupt reduction in the H-dimension of a short length of the ring near the coupling junction. This narrow waveguide is cutoff for the design frequency band. The theory of the offset junction (see below) also tends to indicate that the field intensity at the entrance to this cutoff guide section is greatly reduced due to the out-of-phase cancellation by the two principal modes that can propagate in the junction cavity.

4-1.3. Offset Junction

The offset ring-switch junction[1] was developed at Georgia Tech under Contract Nos. DA 36-039 SC-72789 and DA 36-039 SC-74870. The junction consists of a cavity of length a and width b which is used as a coupling device between two rectangular waveguides as illustrated by a section through a

typical junction in Figure M. The light lines in the upper waveguide represent a mechanical separation which permits relative motion between sections A and B. Use of the junction in the ring switch can be seen in Figure L.

The junction has a simple geometrical configuration which requires no additional matching devices. Its performance is independent of the E-dimension, since all discontinuities are parallel to the E-field. In the junction cavity, the width b, which is approximately one and a half times the width of the coupled guides, is large enough to propagate both the TE_{10} and the TE_{20} modes; the impedance characteristics of the junction result from the interaction of the energy in these modes. A rigorous theoretical analysis of the junction has not been completed; however, the following semi-quantitative analysis serves to indicate the principle of operation.

The offset junction is a bilateral device; however, in this discussion it will be assumed that the energy is coupled from guide 1 into guide 2 (Figure N). At the discontinuity between guide 1 and the cavity, all TE_{mo} modes are excited; however, only the TE_{10} and TE_{20} modes are above cutoff frequency. The TE_{10} mode energy has a lower phase velocity than the TE_{20} mode energy; therefore, their relative phase changes as they propagate down the cavity. If the total relative phase shift in the cavity is π, all of the energy is coupled from guide 1 into guide 2. This situation is illustrated in Figure N; notice that the boundary conditions at the ends of the cavity are roughly satisfied if the phase and amplitude of each mode are as illustrated.

The total relative phase shift in the junction cavity is

$$\theta_r = \theta_{10} - \theta_{20}$$

or

$$\theta_r = 2\pi a_e \left(\frac{1}{\lambda_{g10}} - \frac{1}{\lambda_{g20}}\right)$$

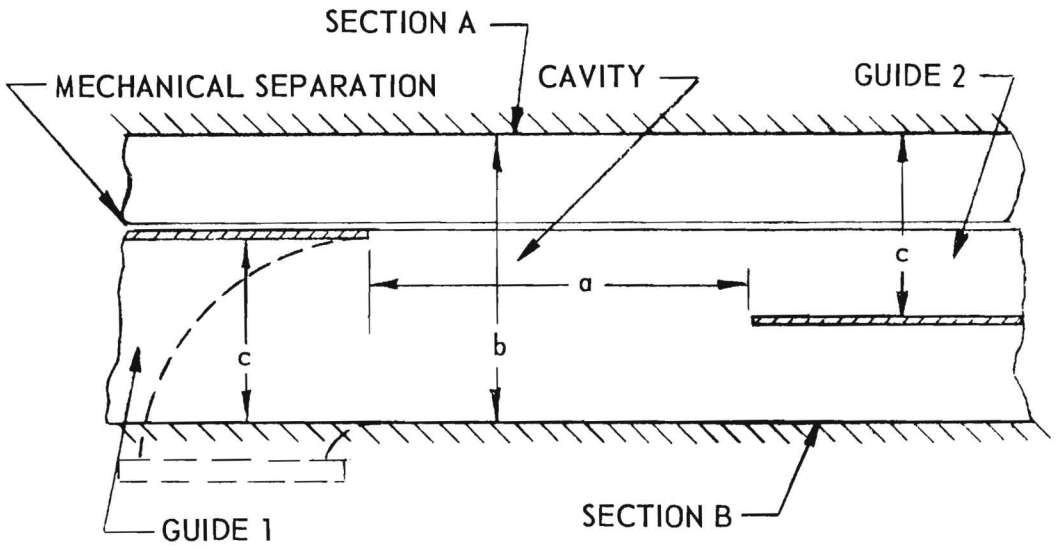

Figure M. The Basic Geometry of the Offset Junction.

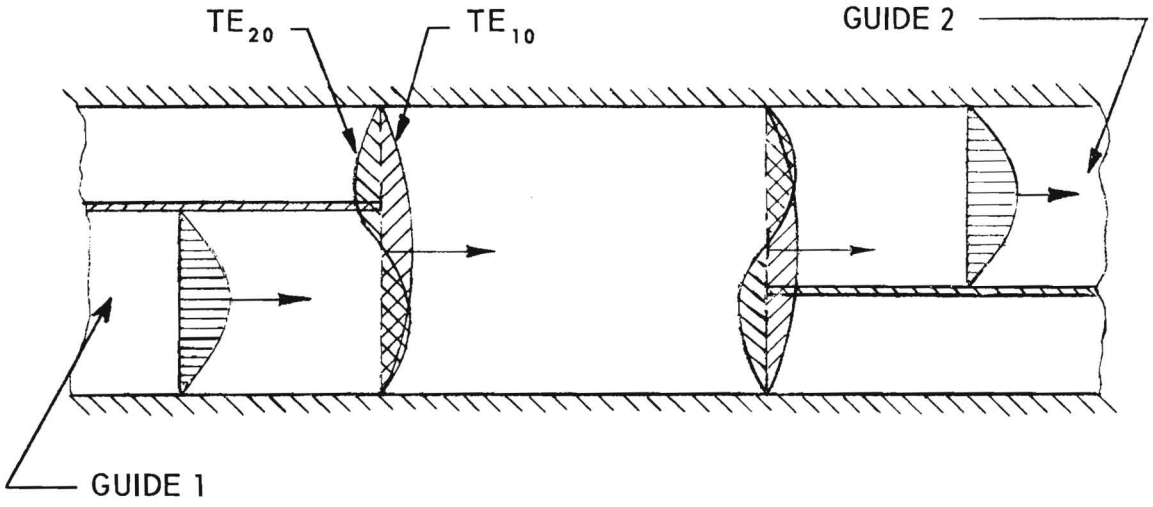

THE CURVES REPRESENT THE E-FIELD AMPLITUDE, AND THE ARROWS REPRESENT THE DIRECTION OF PROPAGATION.

Figure N. The Propagating Modes in the Offset Junction.

where θ_{10} and θ_{20} are the phase changes of the TE_{10} and TE_{20} modes, respectively, a_e is the electrical length of the cavity, and λ_{g10} and λ_{g20} are the guide wavelengths in the cavity for the TE_{10} and TE_{20} modes, respectively. Because of the cavity end effects, the electrical length of the cavity a_e is approximately 13-1/2 percent of a free-space wavelength longer than its physical length a.

In order to have the total relative phase shift between the two modes, after they propagate through the cavity, to be π for proper coupling between the waveguides, the electrical length a_e of the cavity must be n half-wavelengths long for the TE_{20} mode and $n + 1$ half-wavelengths long for the TE_{10} mode, where n is a positive integer; then, the electrical length and the width of the cavity are given by the following equations[1]:

$$a_e = \lambda \left[\frac{3n^2 + 8n + 4}{12}\right]^{1/2}$$

$$b = \lambda \left[\frac{3n^2 + 8n + 4}{8n + 4}\right]^{1/2}$$

λ is the free space wavelength corresponding to a frequency f_o. The calculations for determining the physical dimensions of the offset ring-switch junction are shown in Appendix D.

The cavity has wide bandwidth characteristics centered about the frequency f_o, but, at f_o, a TE_{20} mode resonance has sometimes been found to occur; this resonance can reduce the power handling capacity of the junction at this frequency. Thus, the cavity for the ring-switch junction was designed so that f_o was a frequency located just outside the desired frequency band. One of the factors that makes possible the wide bandwidth characteristics of the junction is the fact that the relative phase shift θ_r between the modes, for a given cavity, remains more nearly constant over a band of frequencies than does the phase shift of either mode.

4-1.4. Curved Offset Junction

Figure M illustrates the manner in which the offset ring-switch junction was split for use in the ring switch. In this case, guide 2 represents the ring guide which was split down the center of the H-dimension. Since the currents in the guide walls are parallel to the split except in the junction cavity, chokes were required only in this region, and the loss in the split ring guide is almost as small as that in ordinary waveguide.

The junction cavity was curved in the E-plane to make possible its application in the ring switch; since the mean cavity length was made equal to that calculated in Appendix D for an uncurved junction, the junction performance was not appreciably affected by the curved configuration. The mean radius of the curved cavity and its associated curved ring guide was made sufficiently large to provide the desired active scan sector for the antenna having four reflectors (see Appendix D).

4-1.5. Waveguide Bends

The mean radius of the input bend, connecting the input junction to the stationary input waveguide, and the mean radius of each of the four output bends, connecting the output junctions to the waveguides extending to the pillbox feeds, were designed to give minimum practical VSWR (see Appendix D).

4-1.6. Electrical Performance

The switch has four output arms spaced 90° apart and activated sequentially through an active azimuthal sector of 40 degrees with the center of the sector adjustable throughout a range of 143 degrees. After the switch had been constructed, electrical measurements were made to determine the electrical characteristics of the switch. The maximum VSWR was measured for representative frequencies over the operating band of 8550 mc to 9550 mc and for various re-

lative orientations of the three junctions located in the three switch sections; this curve is shown in Figure O. The energy transmission path (see Figure L) consisted of the input bend to which was attached a sliding wood load, the input junction, a portion of the lower ring guide, the steerable center-section junction, a portion of the upper ring guide, one of the output junctions, and its associated output bend to which was attached the slotted line and the microwave generator. The angular positions of the center ring and the input ring were varied to determine the maximum VSWR at each frequency.

The insertion loss through the entire ring switch was measured by the substitution method and found to be less than 1/5 db at 9050 mc; the loss increased slightly near the upper edge of the design band.

A high power source was not available so it was not possible to determine the power-transmitting capability of the switch.

4-2. Waveguide

In the construction of the original MILORD antenna, RG-52/U waveguide was used. Since the theoretical power-transmitting capacity for this waveguide (over the present design band of 8550 mc to 9550 mc) would have been limited to 223 kw with a safety factor of 2, the RG-52/U waveguide was replaced with RG-51/U which increased the power capacity of the antenna to 422 kw (see Appendix E). In order to install the larger waveguide it was necessary to modify the primary-feed supporting structure to provide additional mechanical clearances. All waveguide bends, employed in the antenna and the ring switch assembly, possessed mean radii that had been calculated to give them minimum practical VSWR at the design frequency of 9050 mc and low VSWR over the 1000 mc bandwidth (see Appendix D for the equations used).

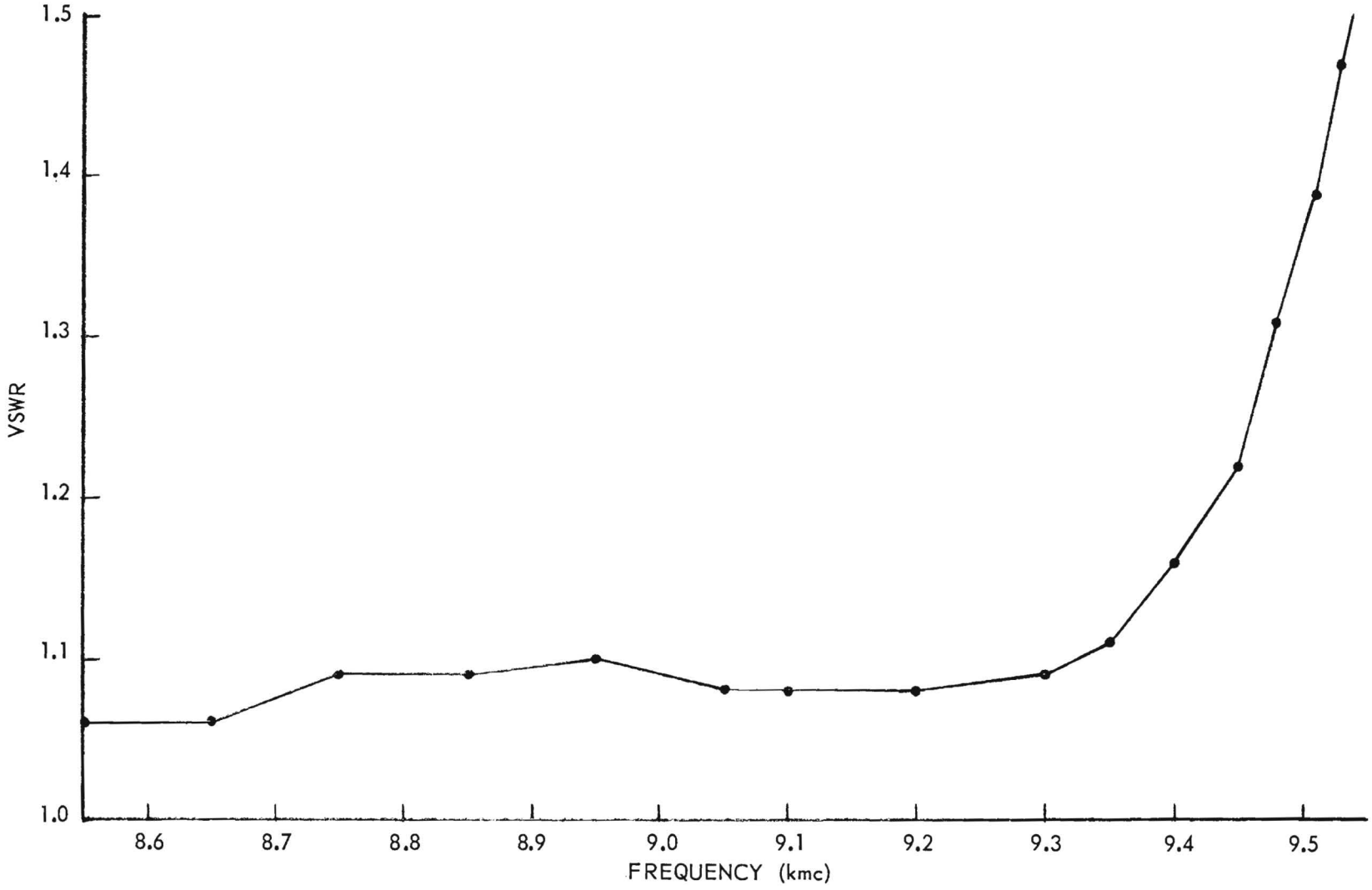

Figure 0. Maximum VSWR Versus Frequency Curve for the Ring Switch.

V. SCAN-SECTOR STEERING MECHANISM

A remotely-controlled motor-driven steering mechanism is located on the trailer beneath the scanning antenna and inside its spindle; on command, it relocates the scan sector of the antenna to any desired position within the limits of its steerable sector. This scan-sector steering is accomplished by the rotation of the center section of the ring switch in proper synchronization with the sync-unit turntable.

This mechanism consists of a reversible drive-motor, gears, shafts, limit switches, anti-backlash springs, a position-indicating potentiometer, and a turntable for supporting a sync-pulse generating unit. A motor switch, a position-indicating meter, and interconnecting cables are provided for remotely steering the scan sector; limit switches prevent accidental positioning of the scan sector beyond the limits of its steerable sector.

A shaft, rotating at twice the antenna speed and in the reverse direction, is located below the antenna and above the turntable; this shaft can be used to drive a sync-unit mounted on the turntable. The turntable is geared to the center section of the ring switch and, during scan-sector steering, the turntable rotates at four times the speed of the steerable center section of the switch and in the opposite direction.

VI. BALANCING AND ENVIRONMENTAL PROTECTING OF THE ANTENNA

6-1. Balancing of the Antenna

Small variations in the weight and in the symmetry of location of the various components included in the rotating antenna necessitated the balancing of the antenna after its assembly. The antenna, having the outward appearance of a right-circular cylinder free to rotate about its own vertically oriented axis, was mounted on its spindle located on the trailer. As the antenna was slowly being accelerated by its drive motor, a steel pin (temporarily installed in the antenna near its periphery) induced a pulse in a magnetic pickup (attached to the trailer) each time the pin rotated into alignment with the pickup; this pulse was used to initiate the sweep of an oscilloscope. As the antenna and its trailer began to vibrate in a horizontal plane, a "linear-motion" potentiometer (temporarily mounted on a stationary frame and having its actuating rod attached to the trailer through a universal-joint type connection) produced a vertical deflection voltage for the oscilloscope; this voltage was proportional to and synchronized with the vibration of the antenna and trailer in the direction of the movement of the actuating rod of the potentiometer. Thus, the location of the peak deflections of the oscilloscope beam (relative to the location of the pulse that initiated the sweep) indicated the angular position (relative to the location of the steel pin) of a diametrical line on which lay the center of gravity of the unbalanced antenna. The amplitude of the deflection of the beam was proportional to the amplitude of the vibration, and the polarity of the deflection was indicative of the sense of the location of the center of gravity on the above diametrical line.

By the "cut-and-try" method, sufficient equivalent weight was attached diametrically opposite the above location of the center of gravity of the

antenna in order to shift the center of gravity into alignment with the axis of rotation. The center of gravity of the attached weights was maintained equidistant between the upper and lower surfaces of the antenna in order not to produce any additional dynamic unbalance. (Note that the above method only produced a static balance condition which reduced system vibration to a negligible value; the only effect produced by any existing small dynamic unbalance would be a small increase in the radial load on the main bearings of the antenna, and so dynamic balancing was not attempted since the bearings were carrying only a small percentage of their rated load.) It was found that a satisfactory static balance condition was obtained when a beam deflection of negligible amplitude was present on the oscilloscope.

6-2. Environmental Protecting of the Antenna

Considerable effort was devoted to the selection and application of the proper surface coatings for the antenna and the trailer since they were to be installed on the sea coast and subjected to an extremely corrosive environment.

The unpainted aluminum components included in the antenna assembly were thoroughly cleaned and then coated with Iridite No. 14-9 (manufactured by Allied Research Products, Inc., Baltimore, Maryland). These components were the pillbox primary feeds, the cylindrical reflectors, the inside surfaces of the aluminum honeycomb radomes, and the microwave ring switch. Iridite provides a highly corrosive-resistant chromate coating on the surface of aluminum with a minimum effect on its electrical characteristics. A coating of Irilac No. 1000 (also manufactured by Allied Research Products, Inc.) was applied over the Iridite coating to further increase the corrosion resistance of the aluminum surfaces.

The top surface of the antenna was covered with a thick coating of Polysulfide Rubber Sealing Compound No. EC-1239 A-2 (manufactured by the Minnesota Mining and Manufacturing Co., St. Paul, Minnesota). This coating made the surface waterproof, and thus aided in the protection of the interior structural members of the antenna.

The fiberglas honeycomb radomes were cleaned and then coated with Epon No. 815 containing Curing Agent "U" (manufactured by Shell Chemical Corp., New York, N. Y.).

All unpainted steel components associated with the antenna hub, main bearings, and the drive spindle were coated with Shell Ensis Fluid No. 210 rust preventative (manufactured by Shell Oil Company, New York, N. Y.). All other exposed steel members comprising the antenna trailer were painted with Rust-Oleum No. 769 Damp-Proof Red Primer-SO and Rust-Oleum No. 975 Brine-Proof Navy Gray-SO (manufactured by Rust-Oleum Corp., Evanston, Ill.).

VII. INSTALLATION AND OPERATION AT THE FIELD SITE

After completion of the redesign and the development of the MILORD antenna system, it was transported to Boca Raton, Florida, where it was installed at a field site operated by the Naval Research Laboratory. The antenna was placed in operation and was continuing in operation at the time of the preparation of this report.

VIII. CONCLUSIONS

The principal electrical characteristics of the MILORD Antenna, before and after modification, are included in Table I.

Table I

The Principal Electrical Characteristics of the MILORD Antenna Before and After Modification

	Before	After
Azimuth half-power beamwidth (degrees)	0.75	0.74
Elevation half-power beamwidth (degrees)	3.5	3.65
Scan sector (degrees)	85	40
Scan-sector steering angle (degrees)	0	143
Scan rate (scans/sec.)	4, 8 or 16	8 or 16
Polarization	Horizontal	Vertical
One-way gain (db over an isotropic radiator)	40	39
Frequency (mc)	9375	9050
Bandwidth (mc)	190	1000
Peak power (kw)	250	300
Azimuth side-lobe level (db)	- 19	- 17-1/4
Elevation side-lobe level (db)	--	- 21

IX. ACKNOWLEDGEMENTS

The successful completion of this project was made possible through the combined efforts of many of the personnel of the Georgia Tech Engineering Experiment Station and representatives of the Naval Research Laboratory.

Some of the key Georgia Tech personnel who aided in the completion of this contract are listed below along with the approximate number of man-months of effort expended.

Name	Title	Man-months
Bryant, D. J.	Research Assistant	4.6
Butterworth, J. C.	Research Assistant	1.2
Cerny, J. C.	Assistant Research Engineer	1.0
Holliman, A. L.	Assistant Research Professor	7.3
Johnson, R. C.	Research Physicist	1.1
Lafitte, G. A.	Research Engineer	2.9
Lockman, J. E.	Assistant Research Engineer	3.5
Long, M. W.	Special Research Engineer	0.8
Rivers, W. K.	Research Physicist	0.5
Shackelford, R. G.	Research Assistant	5.4

Respectfully submitted,

A. L. Holliman
Project Director

Approved:

M. W. Long, Chief
Electronics Division

J. E. Boyd, Director
Engineering Experiment Station

APPENDIX

LIST OF APPENDICES

APPENDIX A

DESIGN OF THE PILLBOX BARRIER FEED-HORN

The dimensions of the original H-plane horn are shown in Figure P and its radiation pattern is shown in Figure R. The amplitude distribution of the E-field in the aperture of the horn (in a plane parallel to the parallel plates) varied as a cosine function of the distance measured from the center of the aperture (since the E-field was oriented perpendicular to the parallel plates). Although the pattern does not have a narrow beamwidth, the following equation can give a rough approximation for the H-plane beamwidth[2].

$$\theta_H = 1.2\,\frac{\lambda}{a} = \frac{1.2\,(1.26)}{1.704} = 0.886 \text{ radian} = 51.8^\circ$$

θ_H = half-power beamwidth (radians)

λ = wavelength of the field in the medium into which the horn radiates (in.) = 1.260 in. (free-space wavelength for f = 9375 mc since the E-field is perpendicular to the parallel plates)

a = horn aperture dimension measured parallel to the parallel plates (in.)

The measured half-power beamwidth of a full-scale model of the above horn, radiating between parallel plates, was found to be 48.2 degrees (see Figure R); thus, it appeared that the equations[2] derived for narrow-beam antennas can be used to give approximate beamwidths for wide-beam antennas.

The specification of vertical polarization dictated that the E-field in the redesigned pillbox be oriented parallel to the parallel plates (see Figure Q). Thus, the amplitude distribution of the E-field in the aperture of its barrier feed horn (in a plane parallel to its parallel plates) was

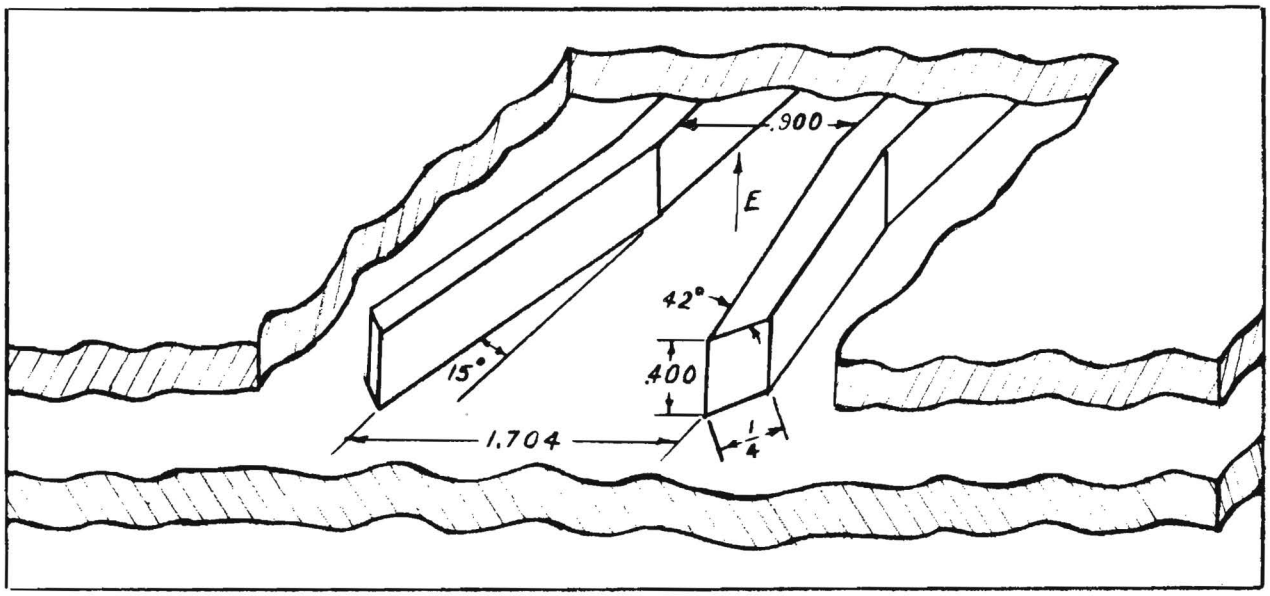

Figure P. Original H-Plane Sectoral Feed Horn for the Parabolic Barrier of the Pillbox.

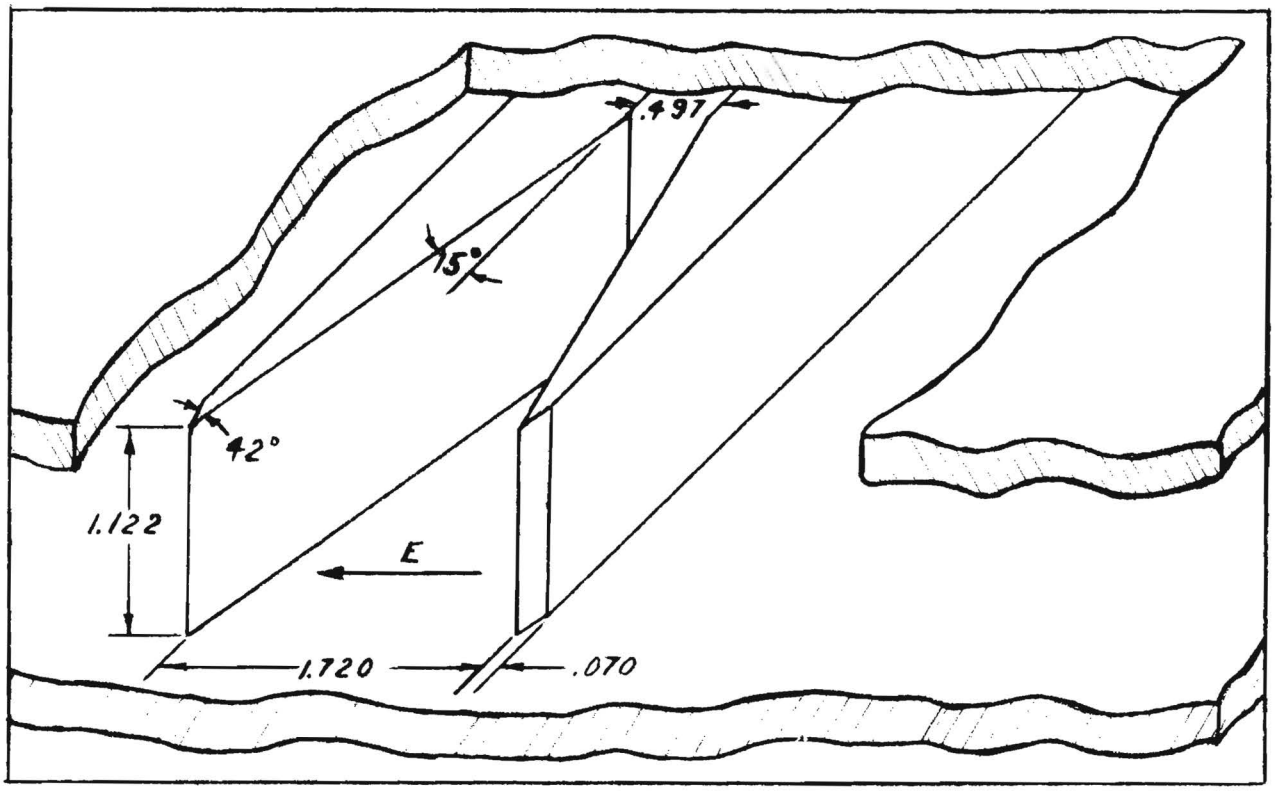

Figure Q. Redesigned E-Plane Sectoral Feed Horn for the Parabolic Barrier of the Pillbox.

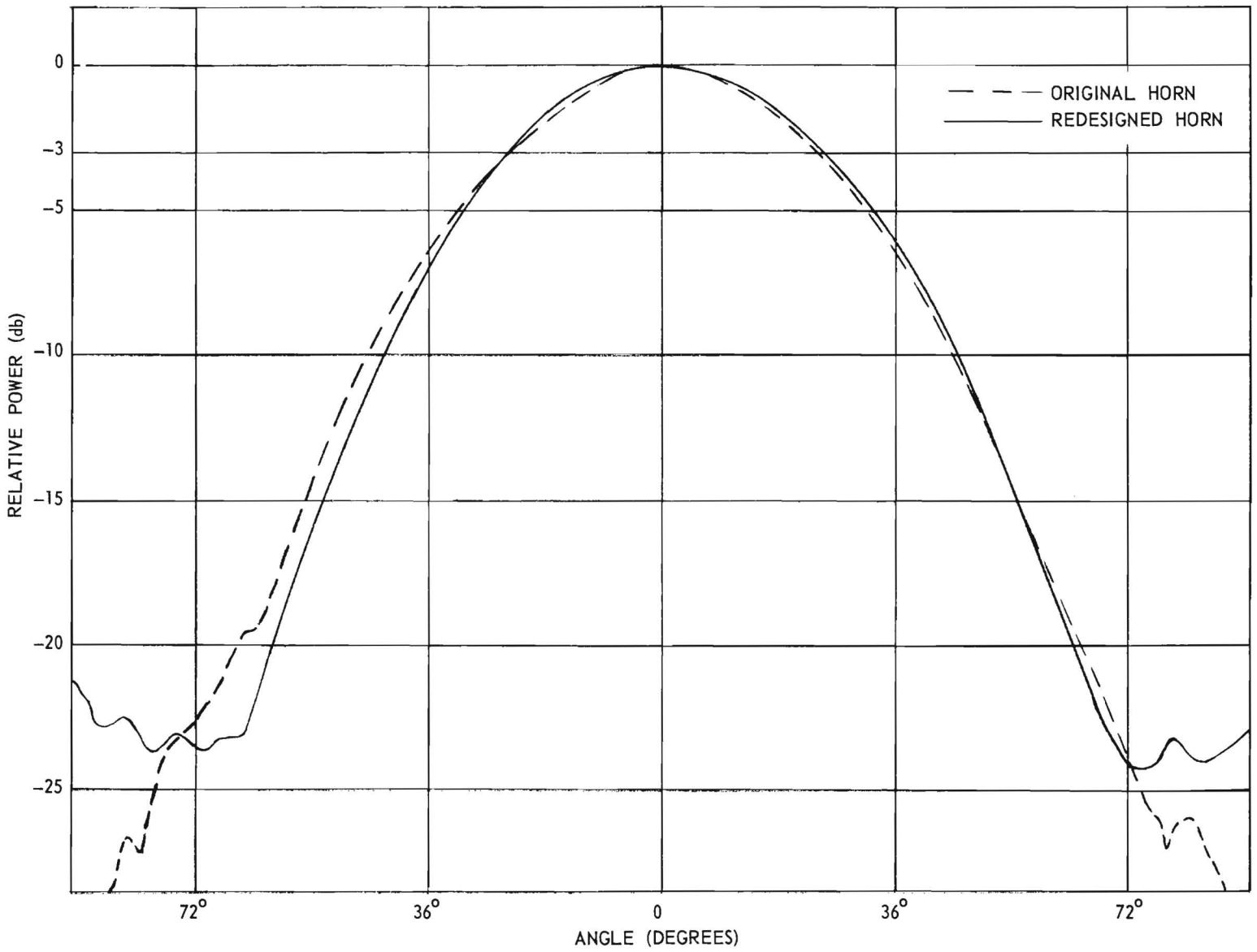

Figure R. Radiation Patterns of the Original Barrier Feed Horn and of the Redesigned Barrier Feed Horn. (Note: Patterns were made in a plane parallel to the parallel plates as the horns radiated between them.)

uniform, and the wavelength of the field between the parallel plates was the same as waveguide wavelength since the plates were spaced 1.122 inches apart (the H-plane dimension for RG-51/U waveguide). Then an approximate value for the half-power beamwidth was obtained from the following equation[2].

$$\theta_E = .88 \frac{\lambda}{a}; \quad a = \frac{.88\lambda}{\theta_E} = \frac{(.88)(1.603)}{(.841)} = 1.677 \text{ in.}$$

θ_E = half-power beamwidth (radians) = .841 radians (for a desired beamwidth of 48.2° that would be equivalent to that of the original H-plane horn)

λ = wavelength of the field in the medium into which the horn radiates (in.) = 1.603 in. (waveguide wavelength for RG-51/U waveguide)

a = horn aperture dimension measured parallel to the parallel plates (in.).

A horn was constructed having this calculated E-plane aperture dimension (1.677 in.) and having a small E-plane flare angle (15° half-angle as was in the original H-plane horn). The radiation pattern of this horn was measured as it radiated between parallel plates; the beamwidth of the pattern was found to be slightly larger than the 48.2° of the H-plane horn. By use of the "cut-and-try" method, the width of the aperture was increased to 1.720 inches which gave a radiation pattern that closely corresponded to that of the original H-plane horn (see Figures Q and R).

APPENDIX B

DESIGN OF THE PILLBOX OUTPUT HORN

The dimensions of a full scale model of a one-inch-high section of the output horn of the original pillbox are shown in Figure S, and its radiation pattern is shown in Figure U. This radiation pattern was measured as it radiated between parallel plates at a frequency of 11,085 mc. (This frequency gave the same wavelength between the plates, with polarization parallel to them, as the free-space wavelength at 9375 mc (1.259 inches) that existed in the vicinity of the aperture of the output horn of the original pillbox.) This frequency was calculated from the following equation[3].

$$\lambda_g = \frac{\lambda}{\left[1 - \left(\frac{\lambda}{2a}\right)^2\right]^{1/2}}$$

λ_g = waveguide wavelength = 1.259 in. (to correspond to free-space wavelength at 9375 mc).

a = H-plane waveguide dimension = 1 in. (spacing between parallel plates).

λ = free-space wavelength for the required impressed frequency.

$$\lambda = \left[\frac{(2a\lambda_g)^2}{4a^2 + \lambda_g^2}\right]^{1/2} = \left[\frac{[2\,(1)(1.259)]^2}{4(1)^2 + (1.259)^2}\right]^{1/2} = 1.0655 \text{ in.}$$

$$f = \frac{v}{\lambda} = \frac{3(10)^{10}}{(1.0655)(2.54)} = 11{,}085 \text{ mc}$$

The 10 db beamwidth of this pattern was approximately 180 degrees. In order to design an H-plane output horn (to provide for vertical polarization) with approximately the same beamwidth, an H-plane aperture of about .53 λ (0.691 in.) would have been required[4].

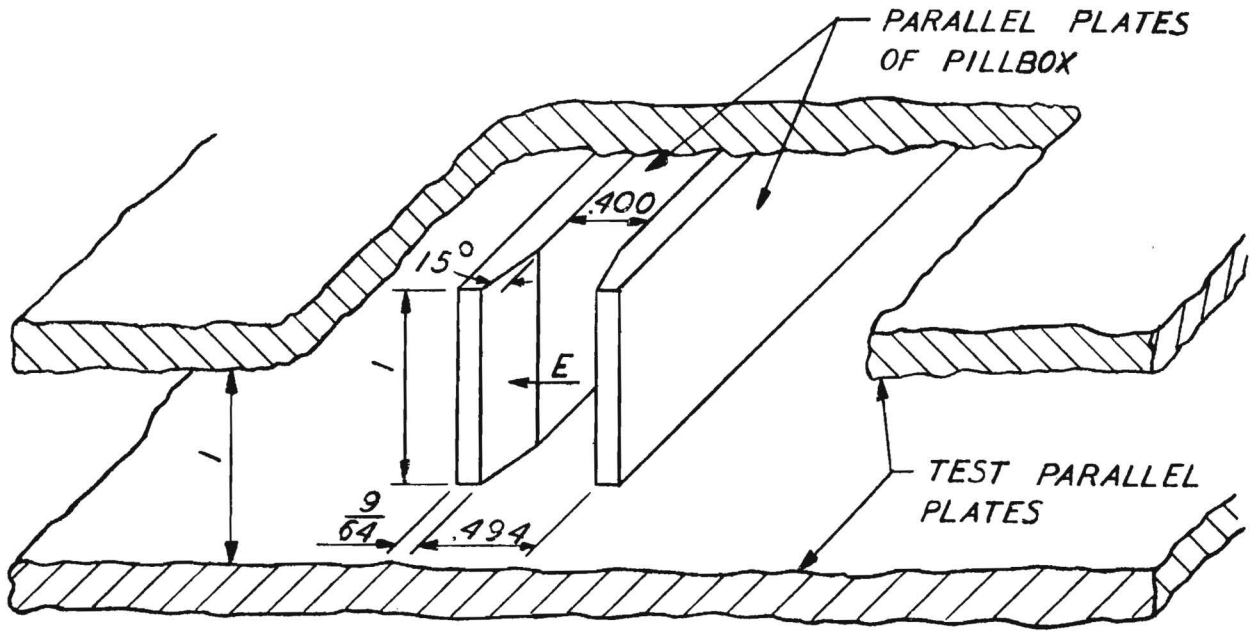

Figure S. A Full-Scale Model of a One-Inch-High Section of the Output Horn of the Original Pillbox. (Note Orientation of the Electric Field).

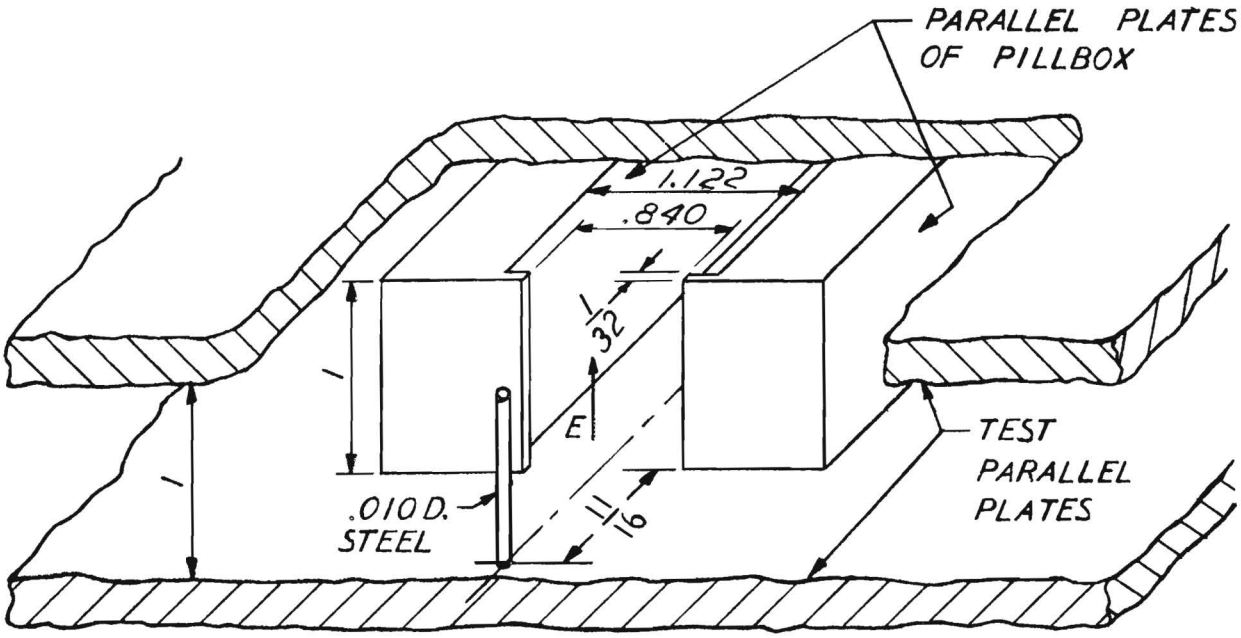

Figure T. A Full-Scale Model of a One-Inch-High Section of the Output Horn of the Redesigned Pillbox. (Note Orientation of the Electric Field.)

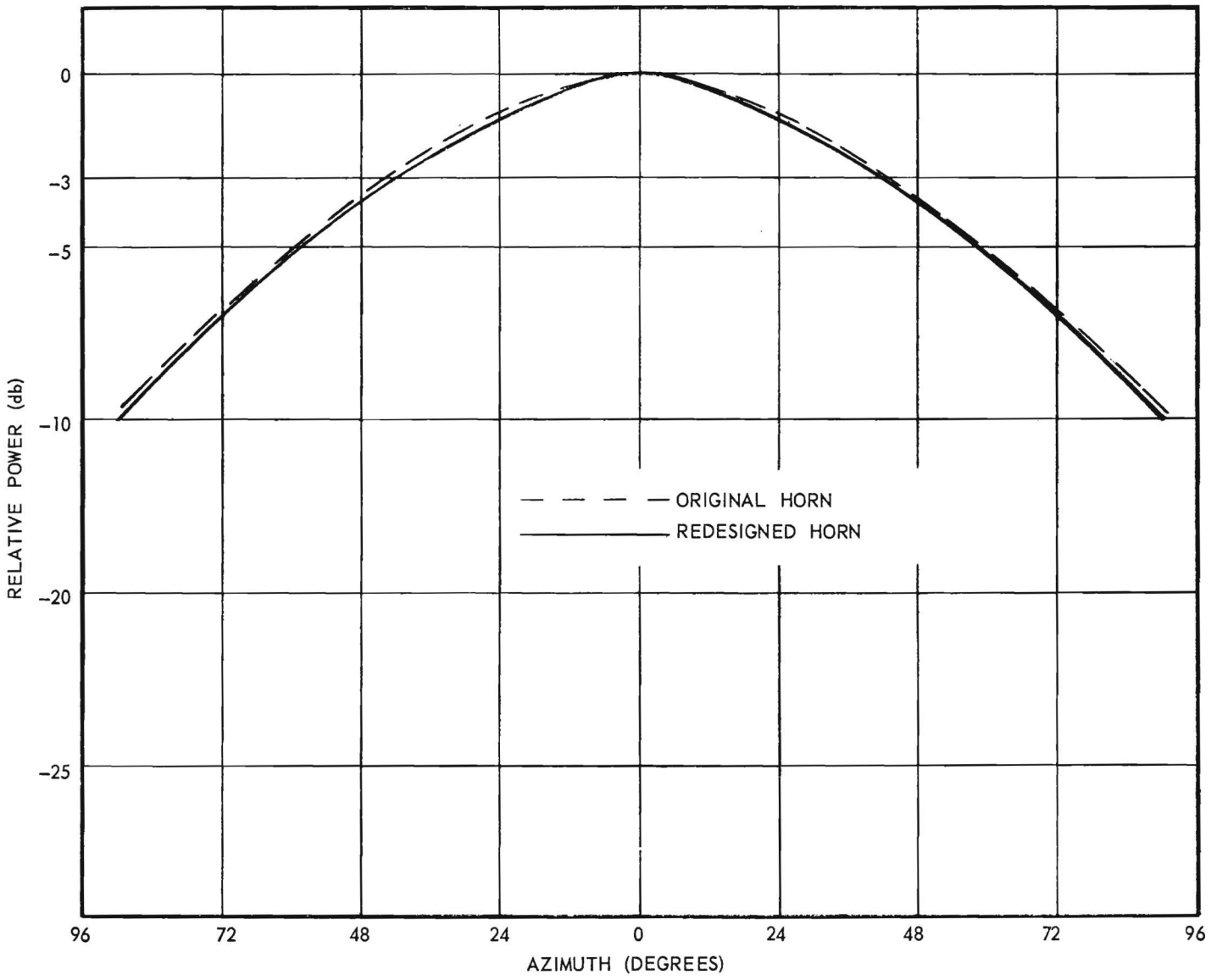

Figure U. Azimuth Radiation Patterns of the Original Pillbox Output Horn and of the Redesigned Output Horn.

$$\theta_H = 31 + 79 \frac{\lambda}{A}$$

$$A = \frac{79\,\lambda}{\theta_H - 31} = \frac{79\,\lambda}{180 - 31} = .53\,\lambda = 0.691 \text{ in.}$$

θ_H = 10 db beamwidth (degrees) = 180° (required to give beam correspondence)

A = H-plane aperture (in.)

λ = free space wavelength of the impressed frequency = 1.304 in. (for f = 9050 mc)

Since the required aperture A of 0.53 λ was very close to the cutoff value of 0.5 λ, and since a long gradual taper would have been required to obtain a low-reflection transition between the parallel plates (spaced 1.122 inches apart) and this aperture, an output horn having this aperture was considered impractical.

It was then decided to obtain the desired wide beamwidth by the combination of two methods;[5] the aperture was abruptly reduced from 1.122 inches to 0.840 inch and a 0.010 inch diameter steel wire was centrally positioned 11/16 inch in front of this aperture (see Figures T and D). The details of this configuration were experimentally determined, and its radiation pattern is shown in Figure U with the original pillbox azimuth radiation pattern.

APPENDIX C

ORIENTATION OF THE PILLBOX BARRIER WITH THE PILLBOX APERTURE

If energy transmission from the pillbox into free space is assumed and a ray path is traced (assuming that the theory of geometrical optics applies), the following details will be observed. The velocity of the ray within the pillbox is greater than that in free space outside the pillbox aperture. The velocity within the pillbox is equal to the velocity in RG-51/U waveguide since the E-field is oriented parallel to the parallel plates which are spaced 1.122 inches apart (the H-plane dimension of RG-51/U waveguide). In order for the ray to emerge at the required angle α with respect to the normal to the aperture (see Section 3-2.2, Reflector Offset Orientation), it must make an incident angle β with the normal. The angle β was calculated from the following equation[6]:

$$\frac{\sin \beta}{\sin \alpha} = \frac{v_g}{v_o} = \frac{f \lambda_g}{f \lambda_o} = \frac{\lambda_g}{\lambda_o}$$

β = angle of incidence (at aperture) inside pillbox

α = angle of refraction (at aperture) outside pillbox = 2° (angle required to give horizontal orientation of main beam of antenna)

λ_g = wavelength inside pillbox = 1.603 in. (waveguide wavelength for RG-51/U for 9050 mc)

λ_o = free space wavelength = 1.304 in. (for 9050 mc).

Then:

$$\sin \beta = \sin \alpha \left(\frac{\lambda_g}{\lambda_o}\right) = \sin 2° \left(\frac{1.603}{1.304}\right) = 0.0429$$

$$\beta = 2.458°$$

Thus, since inside the pillbox the rays propagate in a direction perpendicular to the latus rectum of the barrier, the latus rectum was oriented at an angle

of 2.46° with respect to the pillbox aperture (see Figure C).

APPENDIX D

CALCULATIONS FOR DETERMINING THE PHYSICAL DIMENSIONS OF THE OFFSET JUNCTION AND THE WAVEGUIDE BENDS OF THE RING SWITCH

D-1. The Offset Junction

Since RG-51/U waveguide had been selected as the interconnecting waveguide for the antenna assembly, it was desirable to make dimension c, the H-dimension of the ring guide of the ring switch, the same as the H-dimension (1.122 in.) of RG-51/U in order to avoid the need for a tapered section of waveguide at the input and output of the switch (see Figure V). The dimension e, the mechanical separation between the stationary and the movable sections of the switch, was assumed to be 0.006 inch. (Although an absolute minimum possible separation would have been desirable to prevent small energy losses due to radiation through the separation slot, it was believed that 0.006 inch was the minimum practical separation that could be obtained without the possibility of physical contact and interference existing due to machining and assembly tolerances.) The dimension d should be as small as practical (0.020 in. - 0.040 in.) without being dimensionally unstable.

Then from Figure V,

$$b = \frac{c}{2} + \frac{e}{2} + d + c = \frac{1.122}{2} + \frac{.006}{2} + d + 1.122$$

$$b = d + 1.686$$

but[1]

$$b = \lambda \left[\frac{3n^2 + 8n + 4}{8n + 4}\right]^{1/2}$$

λ is the free space wavelength corresponding to a frequency f_o, and n is a positive integer. Since a TE_{20} mode resonance had sometimes been found to occur at f_o, a value for f_o (9600 mc) was selected such that it was located

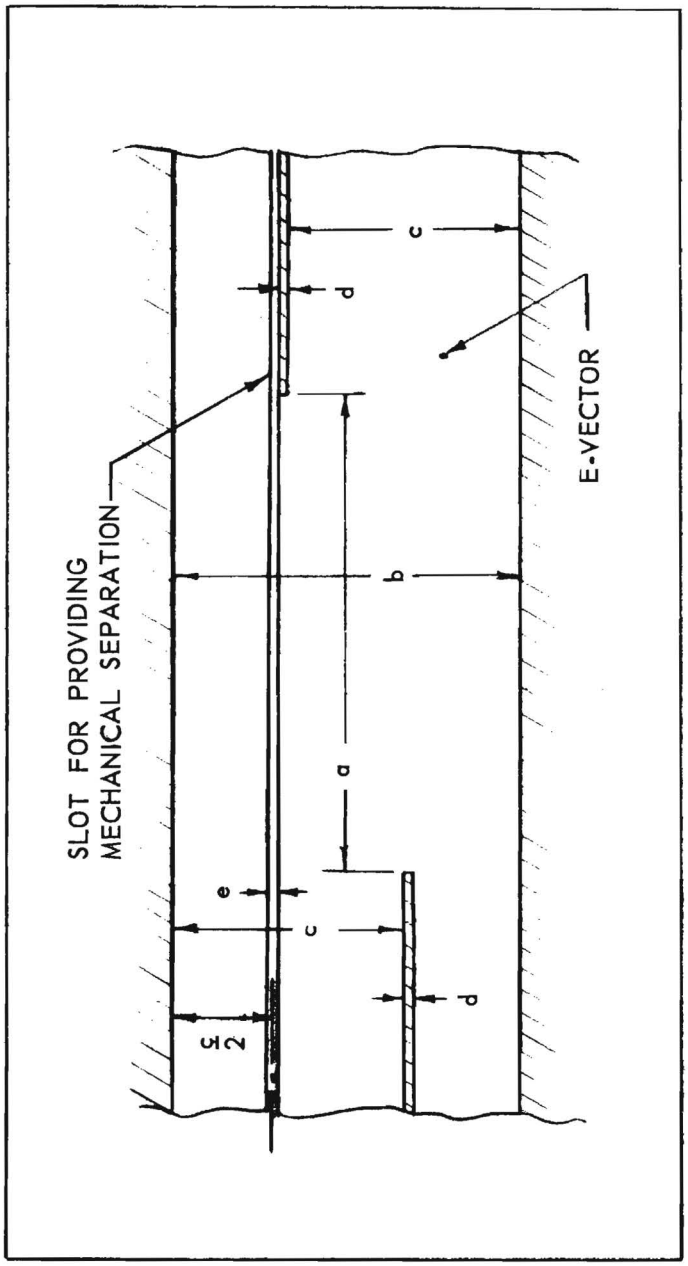

Figure V. Physical Dimensions of an Offset Junction.

just outside the design frequency band of 8550 - 9550 mc. (More recent experimental evidence indicates, however, that the resonances for junctions having dimensions obtained with n = 1, 2, and 3, tend to occur at frequencies which are 0.3, 0.8, and 2.5 percent, respectively, lower than the theoretically predicted value of f_o.)

For

$$f_o = 9600 \text{ mc}$$

$$\lambda = 1.229 \text{ in.}$$

$$d = 1.229 \left[\frac{3n^2 + 8n + 4}{8n + 4}\right]^{1/2} - 1.686$$

which gives

n	d (in)
1	- 0.310
2	- 0.131
3	0.037

Since a value of 3 for n was the smallest possible value, n = 3 was selected for determining the dimensions of the junction. (It was desirable to use the smallest possible value for n in order to obtain a junction with small physical dimensions.)

A standard brass shim-stock dimension for d of 0.032 inch, which was a value near that of the 0.037 inch calculated above, was then selected; the corresponding value of f_o was then calculated to insure its being located outside the design frequency band. (The standard shim-stock facilitated the electroforming of a model of the junction for experimentally checking its electrical characteristics.)

$$\frac{c}{2} + \frac{e}{2} + d + c = b = \lambda \left[\frac{3n^2 + 8n + 4}{8n + 4}\right]^{1/2}$$

$$\frac{1.122}{2} + \frac{.006}{2} + .032 + 1.122 = \lambda \left[\frac{3(3)^2 + 8(3) + 4}{8(3) + 4}\right]^{1/2}$$

λ = 1.2258 in.

f_o = 9635 mc

b = 1.718 in.

Since f_o was located outside the design frequency band, the above dimensions for the junction were considered acceptable.

The dimension a was then calculated.

$$a_e = \lambda \left[\frac{3n^2 + 8n + 4}{12}\right]^{1/2} = 1.2258 \left[\frac{3(3)^2 + 8(3) + 4}{12}\right]^{1/2} = 2.6243 \text{ in.}$$

But it had been experimentally determined[1] that the physical length a of the junction is approximately 13.5 percent λ shorter than the electrical length a_e.

$$a = a_e - .135\lambda = 2.6243 - (.135)(1.2258) = 2.459 \text{ in.}$$

The calculated dimensions for the junction were

a = 2.459 in. (later reduced to 2.303 in.; see below)

b = 1.718 in.

c = 1.122 in.

d = 0.032 in.

e = 0.006 in.

When the electrical characteristics of a full-scale electroformed model of the junction having the above dimensions had been measured, a resonant spike was found to occur in the VSWR-f curve at 9335 mc (see Figure W). The junction length a was reduced until it was experimentally determined that the resonant spike would be located outside the frequency band. For a equal to 2.303 in., the VSWR-f curve shown in Figure W was obtained.

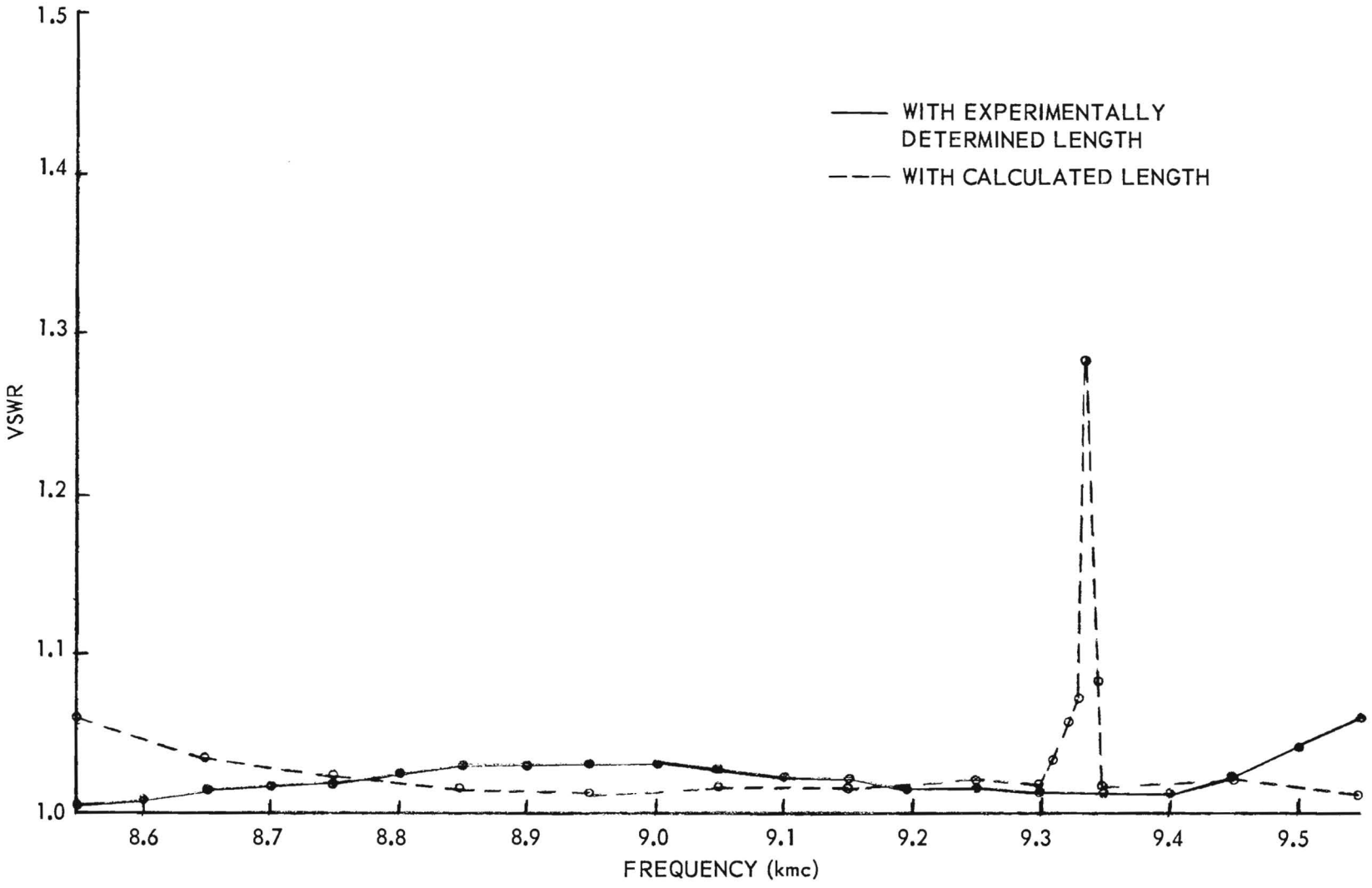

Figure W. VSWR Versus Frequency Curves for an Offset Junction Having the Calculated Length and the Experimentally Determined Length.

D-2. Waveguide Bends

All of the waveguide bends, machined into the microwave ring switch and the pillboxes and electroformed for use in the interconnecting waveguide, were designed with mean radii of curvature that would give minimum VSWR at the design frequency of 9050 mc.

The following equations[11] were used for the calculation of the mean radius of curvature.

For H-plane bends:

$$r_H = \frac{a}{\theta\gamma_{10}} \tan^{-1}\left(\frac{256}{27\pi^2}\,\frac{\gamma_{10}}{-i\gamma_{20}}\right)$$

$$\gamma_{10} = \pi\left[\left(\frac{2a}{\lambda}\right)^2 - 1\right]^{1/2}$$

$$\gamma_{20} = \pi\left[\left(\frac{2a}{\lambda}\right)^2 - 4\right]^{1/2}$$

For E-plane bends:

$$r_E = \frac{a}{\theta\gamma_{10}} \tan^{-1}\left(\frac{96}{\pi^4}\,\frac{\gamma_{10}}{-i\gamma_{11}}\right)$$

$$\gamma_{10} = \pi\left[\left(\frac{2a}{\lambda}\right)^2 - 1\right]^{1/2}$$

$$\gamma_{11} = \pi\left[\left(\frac{2a}{\lambda}\right)^2 - 1 - \left(\frac{a}{b}\right)^2\right]^{1/2}$$

where

θ = angle turned through by the bend

λ = free-space wavelength

a = H-plane dimension of waveguide

b = E-plane dimension of waveguide

r_H = mean radius of curvature for H-plane bend

r_E = mean radius of curvature of E-plane bend

APPENDIX E

CALCULATIONS FOR DETERMINING THE MAXIMUM POWER-TRANSMITTING CAPABILITY FOR RG-52/U AND RG-51/U WAVEGUIDES

Calculations were made to determine if it would be necessary to replace the RG-52/U waveguide installed in the original MILORD antenna with RG-51/U in order to make possible the transmission of 300 kw peak power[7]. Information was not available concerning the width or the repetition rate of the power pulses to be transmitted by the antenna; therefore, power calculations were made on the basis of c-w transmission. It was assumed that the antenna would be operated near sea-level and under an absolute pressure of one atmosphere and that the system VSWR would be very small.

$$W = \frac{a\ b\ E^2}{4\ K_z}$$

W = maximum peak power-transmitting capacity for waveguide (watts)

a = H-plane inside dimension of waveguide (in.)

b = E-plane inside dimension of waveguide (in.)

E = breakdown field intensity (30,000 v/cm = 76,200 v/in. in air at atmospheric pressure)

$$K_z = \frac{\eta}{\left[1 - \nu^2\right]^{1/2}} = \frac{\eta}{\left[1 - \left(\frac{f_c}{f}\right)^2\right]^{1/2}}$$

η = intrinsic impedance of propagating medium in waveguide (377 ohms for air)

f_c = cutoff frequency for the waveguide (mc)

f = impressed frequency (mc)

For RG-52/U waveguide,

a = 0.900 in.

b = 0.400 in.

E = 38,100 v/in. (using a factor of safety of 2)

$$f_c = 6560 \text{ mc}$$

$$W = \frac{a\, b\, E^2}{4\eta \left[1 - \left(\frac{f_c}{f}\right)^2\right]^{1/2}} = \frac{(0.900)\,(0.400)\,(38{,}100)^2}{\frac{4\,(377)}{\left[1 - \left(\frac{6560}{f}\right)^2\right]^{1/2}}}$$

for

$$f = 8550 \text{ mc to } 9550 \text{ mc}$$

$$W = 223 \text{ kw to } 252 \text{ kw}$$

For RG-51/U waveguide,

$$a = 1.122 \text{ in.}$$

$$b = 0.497 \text{ in.}$$

$$E = 38{,}100 \text{ v/in. (using a factor of safety of 2)}$$

$$f_c = 5260 \text{ mc}$$

$$W = \frac{a\, b\, E^2}{4\eta \left[1 - \left(\frac{f_c}{f}\right)^2\right]^{1/2}} = \frac{(1.122)\,(0.497)\,(38{,}100)^2}{\frac{4\,(377)}{\left[1 - \left(\frac{5260}{f}\right)^2\right]^{1/2}}}$$

for

$$f = 8550 \text{ mc to } 9550 \text{ mc}$$

$$W = 422 \text{ kw to } 448 \text{ kw}$$

From the above calculations, it was evident that the RG-52/U waveguide could not transmit 300 kw and so it was replaced with RG-51/U waveguide.

Calculations were made to determine the maximum VSWR (σ) that could be permitted to exist in the RG-51/U waveguide without voltage breakdown when 300 kw of c-w power was being transmitted[8].

$$\sigma = \frac{E_{max}}{E_{min}} = \frac{E_{max}}{|E_i| - |E_r|} = \frac{|E_i| + |E_r|}{|E_i| - |E_r|}$$

σ = voltage standing wave ratio in the waveguide

E_{max} = maximum field intensity

E_{min} = minimum field intensity

E_i = incident field intensity

E_r = reflected field intensity

which gives:

$$|E_i| = \frac{E_{max}}{2} \left(1 + \frac{1}{\sigma}\right)$$

and since P (power) is proportional to E^2

$$P_i = \frac{P_{max}}{4} \left(1 + \frac{1}{\sigma}\right)^2$$

and for 300 kw c-w transmitted power and 422 kw maximum c-w permissible power in RG-51/U within the design frequency band,

$$300 = \frac{422}{4} \left(1 + \frac{1}{\sigma}\right)^2$$

$$\sigma = 1.47 \text{ (VSWR)}$$

Therefore, 300 kw of c-w power could be transmitted through RG-51/U waveguide without voltage breakdown even if the VSWR (σ) were as large as 1.47.

APPENDIX F

ANTENNA GAIN DETERMINATION

F-1. Estimated Gain

An estimate of the gain of the antenna, relative to an isotropic radiator, was made by using calculations employing the measured azimuth and elevation beamwidths.[9]

$$G = \frac{30{,}000}{\theta_E \, \theta_A}$$

G = power gain relative to an isotropic radiator

θ_E = half-power elevation beamwidth (degrees) = 3.65°

θ_A = half-power azimuth beamwidth (degrees) = 0.74°

$$G = \frac{30{,}000}{(3.65)(.74)} = 11{,}100 = 40.5 \text{ db}$$

The reduction in gain that resulted when the radome was installed was measured and found to be less than 1/3 db.

The maximum VSWR that was measured for the antenna assembly was less than 1.2; so assume a 1.2 value for the maximum VSWR. Then the power reflected would be given by[10]

$$\frac{P_r}{P_i} = \left(\frac{\sigma - 1}{\sigma + 1}\right)^2 = \left(\frac{1.2 - 1}{1.2 + 1}\right)^2 = .825 = -.84 \text{ db}$$

P_r = reflected power

P_i = incident power

σ = voltage standing wave ratio

Therefore, an estimate of the actual antenna gain (neglecting the small attenuation due to the flow of currents in the highly conductive metal surfaces of the pillbox, reflector, and the pillbox input-waveguide) would be

$$G_A = 40.5 - .33 - .84 = 39\text{-}1/3 \text{ db.}$$

F-2. Measured Gain

The gain of the antenna was experimentally compared with that of a pyramidal horn having a gain of 15.5 db (above that of an isotropic radiator); the gain of the antenna was 23.6 db above that of the horn. Thus, the measured gain of the antenna was

$$G_M = 15.5 + 23.6 = 39.1 \text{ db.}$$

X. REFERENCES

1. Johnson, R. C., A. L. Holliman, and J. S. Hollis, "A Waveguide Switch Employing the Offset Ring-Switch Junction," I.R.E. Transactions on Microwave Theory and Techniques, Vol. MTT-8, pp. 532-7 (September 1960).

2. Silver, S., Microwave Antenna Theory and Design. New York: McGraw-Hill Book Company, Inc., 1949, p. 187.

3. Marcuvitz, N., Waveguide Handbook. New York: McGraw-Hill Book Company, Inc., 1951, p. 62.

4. Silver, op. cit., p. 365.

5. Ibid., pp. 380-3.

6. Rossi, Bruno, Optics. Reading, Mass.: Addison-Wesley Publishing Company, Inc., 1957, pp. 366-71.

7. Southworth, George C., Principles and Application of Waveguide Transmission. Princeton, N. J.: D. Van Nostrand Company, Inc., 1950, Chaps. 5 and 7.

8. Moreno, Theodore, Microwave Transmission Design Data. New York: Dover Publications, Inc., 1958, Chap. 2.

9. Reference Data for Radio Engineers, 4th Ed. New York: International Telephone and Telegraph Corporation, 1956, p. 704.

10. Moreno, op. cit., p. 25.

11. Rice, S. O., "Reflections from Circular Bends in Rectangular Waveguide," Bell System Technical Journal, Vol. 27, p. 305 (1948).